Spatiotemporal Clusters of ERK Activity Coordinate Cytokine-induced Inflammatory Responses in Human Airway Epithelial Cells

Nicholaus L. DeCuzzi[1,2], Daniel Oberbauer[1], Kenneth J. Chmiel[2], Michael Pargett[1], Justa M. Ferguson[1], Devan Murphy[1], Amir A. Zeki[2,3,4,#], and John G. Albeck[1,#,*].

Affiliations:

[1]Department of Molecular and Cellular Biology, University of California, Davis.

[2]School of Medicine; Department of Internal Medicine; Division of Pulmonary, Critical Care, and Sleep Medicine; Lung Center; University of California, Davis.

[3]U. C. Davis Reversible Obstructive Airway Disease (ROAD)[TM] Center.

[4]Veterans Administration Medical Center, Mather, CA.

[#]Co-Senior Authors

*To whom correspondence should be addressed: jgalbeck@ucdavis.edu

Note: Supplemental videos are available in google drive link provided in external data section.

Funding Sources:

American Lung Association IA-628171 & NHLBI R01 HL151983-01A1 (JGA)

R01 HL148715-01A1 (AAZ)

NIH HL007013 (NLD)

A short running head of no more than 50 characters: Spatial ERK dynamics in airway epithelial cells

ABSTRACT

RATIONALE: Spatially coordinated ERK signaling events ("SPREADs") transmit radially from a central point to adjacent cells via secreted ligands for EGFR and other receptors. SPREADs maintain homeostasis in non-pulmonary epithelia, but it is unknown whether they play a role in the airway epithelium or are dysregulated in inflammatory disease.

OBJECTIVES: (1) To characterize the spatial heterogeneity of ERK activity in response to pro-inflammatory ligands, and (2) to assess the effects of pharmacological and metabolic regulators on cytokine-mediated SPREADs.

METHODS: Live-cell ERK biosensor activity and SPREAD events were measured in human bronchial epithelial cell lines (HBE1 and 16HBE) and primary human bronchial epithelial cells (pHBE), in both submerged and biphasic Air-Liquid Interface (ALI) culture conditions (i.e., differentiated cells). Cells were exposed to pro-inflammatory cytokines relevant to asthma and chronic obstructive pulmonary disease (COPD), and to pharmacological treatments (gefitinib, tocilizumab, hydrocortisone) and metabolic modulators (insulin, 2-deoxyglucose) to probe the airway epithelial mechanisms of SPREADs. Phospho-STAT3 immunofluorescence was used to measure localized inflammatory responses to IL-6.

MEASUREMENTS AND MAIN RESULTS: Pro-inflammatory cytokines significantly increased the frequency of SPREADs. Notably, differentiated pHBE cells display increased SPREAD frequency that coincides with airway epithelial barrier breakdown. SPREADs correlate with IL-6 peptide secretion and localized pSTAT3. Hydrocortisone, inhibitors of receptor signaling, and suppression of metabolic function decreased SPREADs and local STAT3 activation.

CONCLUSIONS: Pro-inflammatory cytokines modulate SPREADs in human airway epithelial cells via both secreted EGFR and IL6R ligands. SPREADs correlate with changes in epithelial barrier permeability, implying a role for spatiotemporal ERK signaling in barrier homeostasis and dysfunction during inflammation. The involvement of SPREADs in airway inflammation suggests a novel signaling mechanism that could be exploited clinically to supplement corticosteroid treatment for asthma and COPD.

One Sentence Summary:

We demonstrate that proinflammatory cytokines cause spatiotemporally organized ERK signaling events called “SPREADs” in human airway epithelial cells, correlating with conditions that disrupt epithelial barrier function.

At a Glance Commentary

Scientific Knowledge on the Subject: Airway epithelial cells play a critical role in the innate immune response to pro-inflammatory conditions. This response must coordinate the recruitment of adaptive immune cells and permit their trans-epithelial migration. ERK signaling is required for these events and has been shown to modulate cell fate outcomes via temporally dynamic activity. Pro-inflammatory conditions may therefore rely on spatially and temporally specific ERK signaling to coordinate immune responses. However, the occurrence of spatially localized signaling events in the airway epithelium has not been investigated.

What This Study Adds to the Field: Combining live-cell ERK biosensors with multiple human airway epithelial models, we demonstrate that pro-inflammatory cytokines induce

spatially localized ERK signaling. In addition, we find that the common anti-inflammatory treatments tocilizumab, gefitinib, and hydrocortisone suppress cytokine-induced SPREADs. These findings suggest that localized ERK signaling coordinates the innate immune response via spatially restricted cytokine release and regulation of airway barrier permeability.

INTRODUCTION

Epithelial cells line the mammalian airway and protect the lung from harmful inhaled particles and pathogens. Such insults trigger inflammatory cytokine signaling within the context of respiratory diseases, as exemplified by asthma and chronic obstructive pulmonary disease (COPD) (1–11). In these diseases, signaling within the epithelial layer is dysregulated at a broad level, but how do the behaviors of individual cells contribute to this disruption? Within an epithelial surface, cells can respond independently to cytokines, but multicellular, coordinated cascades of responses serve to efficiently propagate stimuli (12). Such collective, timed behaviors may be essential to elicit innate immune defenses and maintain tissue barrier homeostasis within the airway epithelium.

Extracellular signal-regulated kinase (ERK) is a well-established regulator of epithelial cell behavior with a plurality of functions in wound healing, tobacco smoke reactivity, inflammation, and innate immune responses. ERK plays a role in these behaviors through its effects on cell proliferation, death, epithelial-mesenchymal transition (EMT), and cytokine production (5, 9, 13). Also implicated in previous studies is the integrity of the epithelial barrier itself, which under influence of ERK signaling allows neutrophil influx from sub-epithelial regions across an intact epithelium (14). Given this widespread role in airway disease pathogenesis and the underlying mechanisms, targeting the ERK 1/2 pathway may have therapeutic potential (15, 16).

In many tissues, ERK signaling is highly localized and temporally dynamic (17), but such patterns have not been investigated in the airway. Given ERK's known roles in

the airway epithelium, a possible function for spatially localized ERK signaling is the coordination of cytokine production with epithelial barrier permeability, creating focal points for immune cell entry. Paracrine release of EGFR ligands often causes a unique type of ERK activity localized to regions of 5 to 50 cells (18–20). These spatially localized ERK signaling events have been termed “SPREADs”, for Spatial Propagation of Radial ERK Activity Distributions, and were first described in non-human epithelial cells (18, 19). Since then, SPREADs have been linked to cell fate events in various non-pulmonary epithelial systems, including instances of proliferation (19), cancer cell ejection (21), and apoptosis (20). However, the role of SPREADs in the context of the airway and their modulation by proinflammatory conditions remains unknown. We hypothesized a new function for SPREADs in airway epithelial cells, in which they allow inflammatory stimuli to transiently increase barrier permeability and cytokine production during airway inflammation.

To evaluate the potential role of SPREADs in airway inflammation, several questions must be addressed. First, while secreted EGFR ligands have been implicated in the propagation of ERK activity, it is unknown if secreted pro-inflammatory cytokines such as IL-6 are connected to SPREAD behavior. Second, it will be important to determine if SPREADs are affected by the metabolic environment of the epithelium, as patients with metabolic disorders (obesity, diabetes) are more susceptible to lung inflammation. Finally, determining the effects of known anti-inflammatory treatments such as corticosteroids on SPREAD behavior is needed to establish the clinical relevance of spatial ERK regulation.

To address these gaps in knowledge, we integrated fluorescent biosensors for ERK activity into human airway epithelial cells and collected live-cell ERK activity data in response to pro-inflammatory conditions, with single cell resolution. We demonstrate that SPREADs occur in various airway epithelial cell lines and primary cells, co-localize with secondary IL-6 secretion, and are modulated by metabolic factors and anti-inflammatory drugs. Our findings suggest a spatiotemporally dynamic mechanism underlying airway disease progression and provide insight into the effects of pro-inflammatory cytokines on airway epithelial cell signaling.

METHODS

Human Airway Epithelial Cell Sources

HBE1, a papilloma virus-immortalized human bronchial epithelial cell line originally generated by Dr. James Yankaskas (University of North Carolina, Chapel Hill, NC) (22), was provided by Dr. Reen Wu of University of California, Davis, and was cultured as described in (23). 16HBE14o- (referred to as 16HBE) cells were obtained from Sigma-Aldrich (#SCC150) and cultured in α-MEM (Sigma M2279) + 2mM L-Glutamine + 10% FBS (24). Normal human primary tracheobronchial epithelial cells (pHBE) were isolated from human bronchi and distal trachea obtained from organ donors via the Cooperative Human Tissue Network. pHBE cells were cultured in submerged and air-liquid interface (ALI) culture as described in (25). *See supplemental methods for further details*.

Live Cell Measurement of ERK activity

Figure 1A shows example images of the ERK biosensors ERK-KTR (26), which has a typical dynamic range of 2-2.5 (arbitrary units) and EKAREN4 (27), which has a typical dynamic range of 0.2-0.25 (arbitrary units); the biosensors are further described in (28). ERK-KTR or EKAREN4 biosensors were stably integrated into cells by lentiviral transduction and used to record single-cell ERK activity at 6-minute intervals for 24 hours following treatment (**Sup. Video 1**). For live-cell imaging, cells were deprived of EGF and BNE/FBS for at least 6 hours (following the protocol described in (29)) and then exposed to one of six conditions that were designed to recapitulate various airway inflammatory states (**Table 1**), individual pro-inflammatory cytokines from these conditions, or controls. In certain experiments, cells were fixed and immunofluorescence staining was used to measure pSTAT3 (**Figure 1B**). Single-cell ERK activity was quantified and pulse analysis was performed using MATLAB as described in (30, 31).

Quantification of Spatially Localized ERK Activity

We developed a MATLAB implementation of Automated Recognition of Collective Signaling (ARCOS) (20, 32). Following the ARCOS methodology, ERK pulses detected in time series data were binarized and subsequently clustered with Density Based Spatial Clustering of Applications with Noise (DBSCAN). Cluster labels were tracked using the k-nearest neighbors algorithm to match neighbors of clusters within a given distance between time points (epsilon).

Our implementation expands on ARCOS by using pulse analysis to identify active ERK pulses for binarization, adding automatic estimations of epsilon and the minimum

number of points within epsilon distance of a point for that point to be considered a core point, based on the distributions of the input data and cluster area calculations using MATLAB's native boundary tracing method. Cluster data can be filtered by duration, start time, maximum area, maximum count, mean rate of change of count and mean rate of change of area, effectively narrowing down the pool of spread candidates. We validated our approach by generating synthetic spreads and using Adjusted Rand Indices (ARI) to compare per-timepoint ground truth cluster assignments to ARCOS cluster assignments of varying lifetime and frequency, observing mean per-timepoint ARI values between 0.96 and 0.99.

Trans-Epithelial Electrical Resistance (TEER) Measurement

TEER values were measured in Phosphate-Buffered Saline (with Ca^{2+} / Mg^{2+}) in air-liquid-interface (ALI inserts by Corning, 3460) using a Trans-Epithelial Electrical Resistance Meter (EVOM3 -World Precision Instruments), which was used and optimized according to the manufacturer instructions.

Measurement of Secreted Ligands

Cultured HBE-1 cells were immersed in serum-free media and treated with cytokines IL-1β (10 ng/ml) and IL-6 (10 ng/ml) with media collections at 2- and 12-hour timepoints. Cytokine levels in media, in treated and untreated wells, were measured via a Luminex High Performance custom assay plate (MilliporeSigma, Item no. HCYTOMAG-60K-16) for detection of TNF-α, RANTES, MCP-1, MIP-1α, Eotaxin, and VEGF-A interleukins 1α, 1β, 4, 6, 8, 10, 17A, 17E, 17F, and 18. Cytokine array measurements were made using the Proteome Profiler Human XL Cytokine Array Kit (ARY022B) from R&D systems,

following the manufacturer's instructions.

RESULTS

Airway disease conditions induce dynamic ERK activity in HBE1 cells

To evaluate temporal ERK activity modulated by pro-inflammatory cytokines, we generated HBE1, 16HBE, and primary human bronchial epithelial (pHBE) cells expressing ERK biosensors (**Figure 1, Sup. Video 1**). For live-cell imaging, cells were deprived of EGF and BNE/FBS for at least 6 hours and then exposed to one of six conditions that were designed to recapitulate various airway inflammatory states (**Table 1**), individual cytokines from these conditions, or controls.

Across the treatments, we observed differences in the fraction of cells responding and, in the intensity, and duration of those responses. While the vehicle control induced a minimal response (**Figure 2A**), the canonical growth factor EGF induced a maximal ERK response, which lasted 60 to 120 minutes, with approximately 98% of cells responding to the treatment (**Figure 2B, Figure E1A;** see Methods for details on quantification). After this initial period, mean ERK activity tapered to approximately half-maximal levels for the remainder of the experiment (22 to 24 hours) (**Figure 2B**). The combination of IL-1β, IL-6, and TNF-α induced a strong immediate ERK response, which on average lasted 19 minutes ($P < 0.005$ versus control) with >75% cells responding (**Figure 2C, Figure E1A**). When tested individually, IL-1β or IL-6 treatment elicited initial ERK responses lasting 14 minutes or 19 minutes, respectively (**Figure 2D&E**). While <25% of cells responded to IFN-γ and TNF-α (**Figure 2F, Figure E2A**), responder activity

lasted 38.4 minutes ($P < 0.005$). Most other pro-inflammatory condition groups tested (IL-4/5/9/13, IL-17A/23, or LPS) did not elicit an initial ERK response that was significantly different from the vehicle (negative control) treatment; however, poly I:C treatment induced a delayed initial peak that was variable across experiments (**Figure 2A, Figure E1, Figure E2**).

At the single-cell level, we observed significant heterogeneity in long-term ERK activity profiles under pro-inflammatory cytokines (**Figure 2 - heatmaps, Figure E1**). While vehicle-treated cells displayed only rare sporadic ERK activation (0.08 ERK pulses per hour), EGF-treated cells showed greatly increased mean activity and frequency of ERK pulses (0.51 pulses per hour). Notably, HBE1 cells treated with IL-1β/IL-6/TNF-α, IL-1β, IL-6, TNF-α, IFN-γ/TNF-α, or IFN-γ displayed increased sporadic ERK activation (0.1 to 0.3 pulses per hour), but without strongly increasing the mean ERK activity (**Figure 2 & Figure E2**). Excluding the initial treatment response, we found no statistical differences in pulse duration compared to control conditions (mean pulse duration = 21 minutes; **Figure E1C**).

Pro-Inflammatory cytokines modify SPREADs in airway epithelial cell lines

We next evaluated if the sporadic ERK pulses induced by pro-inflammatory cytokines were spatiotemporally localized. Concentric ERK signaling waves (i.e. SPREADs) were clearly visible in time-lapse images (e.g., **Figure 3A, Sup Video 2**). To evaluate whether SPREAD behavior is modified by pro-inflammatory cytokines, we used a SPREAD detection program (ARCOS; **Figure 3B**) to analyze SPREAD features including frequency of occurrence (SPREADs per hour normalized to mm^2, SPH),

duration, maximum size, and localization of SPREAD events.

HBE1 cells displayed a significant increase in SPREAD frequency, compared to vehicle-treated cells, only when treated with combinations of either IL-1β/IL-6/TNF-α or IFN-γ/TNF-α (**Figure 3C**). To determine which cytokines in the bulk treatment groups caused the increased SPREAD frequency, we tested each cytokine separately. TNF-α, IL-6, IL-1β, or IFN-γ (20 ng/mL) all caused a significant increase in SPREAD frequency compared to their vehicle-treated counterparts (**Figure 3D**). In EGF-treated cells, the detected SPREAD frequency was inconsistent across replicates and thus was excluded from analysis (**Figure E3A; Sup. Video 3**).

In addition to increased frequency of SPREADs, the average sizes of SPREADs were significantly larger in IL-1β/IL-6/TNF-α and IFN-γ/TNF-α treated cells (1500μm^2 and 1600μm^2) compared to vehicle control (600μm^2) (**Figure E3B**). However, despite heterogeneity in the duration of SPREADs within each condition, no condition displayed a significantly different mean SPREAD duration compared to control conditions (means ranging from 20 minutes to 25 minutes, with a 22 minute average, **Figure E3C**).

To evaluate SPREADs in an alternate epithelial model, we performed a similar analysis in 16HBE cells and observed both common features in SPREAD behavior as well as notable differences. As with HBE1 cells, 16HBE responded with an initial peak of ERK activity when stimulated by EGF, IL-1β/IL-6/TNF-α, or IL-1β stimulation (**Figure 4A-D**). However, 16HBE cells did not display a strong ERK response to IL-6 or IFN-γ/TNF-α (**Figure 4E&F**). A delayed response to Poly I:C, beginning 1 hour after treatment was also present (**Figure 4G**). Also consistent with HBE1 cells, 16HBE cells did not respond

to IL-4/5/9/13, IL-17A/23, or LPS (**Figure E4**). At the single-cell level, individual 16HBE cells displayed sporadic peaks of ERK activity over extended treatment times, and many of these peaks were organized as SPREADs (**Figure 4 - heatmaps**). However, 16HBE cells displayed a higher basal SPREAD frequency compared to HBE1 cells. Against this higher baseline frequency, only TNF-α or Poly I:C induced a significant increase in SPREAD frequency, while IL-6 and IL-1β did not (**Figure 4H**).

The difference in baseline ERK activity between HBE1 and 16HBE cells' behavior could arise from various factors, as the two cell lines differ in their gene expression, in their ability to differentiate into ciliated epithelial cells, and in their standard growth medium composition (22, 24). Notably, HBE1 growth medium contains hydrocortisone, insulin, cholera toxin, and transferrin while 16HBE growth medium does not. These components could feasibly impact the behavior of inflammatory conditions. By visual inspection, we also noted that many of the SPREADs in 16HBE cells appeared to be initiated by apoptosis events (**Sup Video 4**). Consistent with this observation, gefitinib treatment, which blocks apoptosis-induced SPREADs in other systems, ablated basal SPREADs observed in 16HBE cells (**Figure E5**). Overall, results from 16HBE cells corroborate the modulation of SPREADs by inflammatory conditions as observed initially in HBE1 cells, notwithstanding several differences that are potentially explainable by the variations in culture conditions.

Pro-inflammatory cytokines cause spatially coordinated ERK signaling in primary human airway epithelial cells

To extend our findings to a more physiologically representative setting, we introduced the ERK biosensor to primary human bronchial epithelial (pHBE) cells and measured their response to control and pro-inflammatory conditions. As expected, pHBE cells in submerged culture (i.e. not differentiated in ALI culture) did not exhibit a response to vehicle control but displayed a strong ERK response to EGF (10 ng/mL), which validated biosensor function in primary human airway epithelial cells (**Figure 5A&B**). pHBE cells in submerged culture also displayed transient ERK activation in response to IL-1β/IL-6/TNF-α, IL-1β (10 ng/mL and 20 ng/mL), IL-6 (20 ng/mL), and Poly I:C (20 μg/mL) (**Figure 5C-G**). However, pHBE cells did not respond to IL-4/5/9/13, IL-17a/23, or LPS, as seen in both immortal cell lines (**Figure E6**) We noted that IL-1β treatment caused spatially coordinated wave-like ERK activation across the entire image field, lasting 4 hours on average (**Sup. Video 5**). These large waves were not quantifiable as SPREADs since they usually do not originate within the image frame, but they suggest that primary airway epithelial cells respond in an even more coordinated manner than the cell line models.

To investigate the effect of SPREADs on airway epithelial barrier permeability, we measured the ERK response of primary cells after differentiation in air liquid interface culture (ALI) for >30 days; differentiation was confirmed by the presence of beating cilia (**Sup. Video 6**). When treated with 20 ng/mL IL-1β, ALI-differentiated pHBE cells displayed an immediate, uniform ERK response that lasted 2 hours (**Figure 6 - Timelapse Images, Sup Video 7**). Subsequently, SPREADs were clearly observed in all

conditions, with an increased frequency of SPREADs when cells were treated with IL-1β compared to control (**Figure 6C**). Measuring the airway barrier permeability in these samples, we observed a decrease of 19% in epithelial barrier resistance as compared to control, which was not seen in EGF treated cells (**Figure 6D**). This correlation is consistent with our hypothesis that pro-inflammatory cytokines cause increased airway barrier permeability via increased SPREAD events.

Secreted IL-6 signaling plays a significant role in IL-1beta-mediated SPREADs

To establish which secreted ligands generate SPREADs, we measured cytokine abundance in conditioned media from HBE1 cells treated with IL-1β (20 ng/mL) for 12 hours. In cytokine microarray assays, GROα, IL-17A, IL-6, IL-8, MCP-1, IL-8, and MIP3α , were all increased at least 1.5-fold by IL-1β (**Figure 7A**). We cross-referenced this list of cytokines with RNA-seq data from HBE1 cells to identify ligand-receptor pairs that might cause downstream ERK activation, and thereby SPREADs, when secreted. Our analysis showed that IL6R and gp130 had the highest expression amongst the receptor candidates, prioritizing IL-6 as a potential candidate that is further supported by multiple reports in the literature (33, 34). Bead-based cytokine assays further confirmed IL-6 secretion in IL-1β-treated HBE1 cells (**Figure E7**).

As IL-6 can activate ERK through IL6R mechanisms that are EGFR-dependent (35, 36) and EGFR-independent, (35, 37) we sought to determine if the mechanism of ERK activation in SPREADs was unimodal (acting through EGFR or IL6R alone) or multimodal (via multiple receptors). We treated cytokine-exposed HBE1 cells with inhibitors of EGFR or IL6R (gefitinib and tocilizumab, respectively; **Figure 7B**). HBE1 cells

treated with IL-1β and gefitinib or tocilizumab displayed significantly fewer SPREAD events, compared to IL-1β alone. This effect suggested that IL1β-mediated SPREADs are caused via both EGFR and IL6R ligands. However, IFN-γ-induced SPREAD frequency was reduced significantly by gefitinib, but not by tocilizumab, indicating that IFN-γ-mediated SPREADs are primarily EGFR-dependent (**Figure 7B**). Interestingly, tocilizumab or gefitinib treatment significantly decreased IL-6-induced SPREADs, further implying that some SPREADs depend on both EGFR and IL6R activity (**Figure 7B**).

To further investigate the role of IL-6 in spatially localized signaling events, we performed immunofluorescence for phosphorylated STAT3 (pSTAT3), the transcription factor canonically activated by IL-6. As expected, we observed minimal pSTAT3 in control-treated HBE1 cells (**Figure 7C**) while IL-6-treated conditions displayed uniform high STAT3 activation (**Figure 7D**). However, under SPREAD-promoting conditions (IL-1β or IFN-γ), we observed clusters of cells with STAT3 activation which were similar in size and shape to SPREADs (**Figure 7E&F; Outlined by white boxes**). Together, the secretion of IL-6, the dependence of SPREADs on IL6R, and the co-occurrence of pSTAT3 indicate that IL-1β-induced SPREADs in airway epithelial cells are markedly dependent on IL-6 signaling, in addition to the known role of EGFR found in other epithelia.

Metabolic suppression limits cytokine-induced SPREAD frequency

Patients with inflammation-related metabolic syndromes, including diabetes and obesity, show reduced capacity for mucosal barrier repair and are at greater risk for airway barrier-related inflammation (38–43). Considering this comorbidity, we

investigated the impact of metabolic regulators on cytokine-induced SPREADs in our HBE1 cells. To verify elevated metabolic stress, we introduced a second fluorescent biosensor for AMP-activated protein kinase (AMPK) into our HBE1 cells expressing the ERK biosensor (**Figure 8A**). AMPK responds to changes in cellular energetic status and may limit cytokine production when active (44, 45), potentially suppressing cytokine-induced SPREADs.

We first explored how insulin deprivation affected cytokine-induced SPREADs and AMPK activity in our HBE1 cells. Insulin deprivation significantly reduced the frequency of pro-inflammatory cytokine-induced SPREADs (**Figure 8B**). Specifically, we noted that insulin-starved cells treated with IL-1β (10 ng/mL or 20 ng/mL), or IL-6 (20 ng/mL) displayed 47%, 82%, and 26% fewer SPREADs relative to their insulin-treated counterparts ($p < 0.05$ versus control). To further investigate the idea that metabolic stress decreases cytokine-induced SPREADs, we treated the cells with 2-deoxyglucose (2-DG), an inhibitor of glycolysis, to cause maximal metabolic stress. 2-DG treatment induced maximal AMPK activity, indicating high metabolic stress in the cells (**Figure E8**). 2-DG treatment led to a significant (>75%) decrease in IL-6-, high IL-1β-, and low IL-1β- induced SPREAD frequency, when compared to the vehicle-treated counterparts for each cytokine (**Figure 8C**), further indicating that increased metabolic activity correlates with higher SPREAD frequency.

Corticosteroids suppress SPREADs

Corticosteroids such as hydrocortisone are common anti-inflammatory drugs used clinically (46, 47). Their activity is attributed to multiple mechanisms, including suppressed secretion of IL-6 and other pro-inflammatory cytokines (48, 49) and reduced glycolytic metabolism (50). As our previous results implicate both IL-6 secretion and glycolytic metabolism in the promotion of SPREADs, we tested the effect of HC on cytokine-induced SPREADs. We compared HBE1 cells pretreated for 24 hours with 0.5 μg/mL HC (1.38 μM) to cells grown without HC for 24 hours. HC-treated cells were much less susceptible than untreated cells to SPREADs induced by TNF-α and IL-1β with reductions in SPREAD frequency of 80% and 71%, respectively (**Figure 9A**). Together with the higher SPREAD frequency found in 16HBE cells, which as noted earlier are cultured in the absence of HC, these data indicate that HC potently suppresses cytokine-mediated SPREAD activity.

DISCUSSION

There is a pressing need to better understand inflammatory mechanisms in airway epithelial cells that lead to chronic disease pathogenesis and progression. Our data offer deeper insight into the long-standing question of ERK's dual role as a pro- and anti-inflammatory signaling kinase, revealing for the first time intricate spatial patterns of ERK activity (SPREADs) within airway epithelial cells. Specifically, we establish that pro-inflammatory environments promote spatially *localized* ERK activity in the form of SPREADs, whereas growth factor treatment causes more uniformly *distributed* ERK

activity across all measured airway epithelial cells. This difference indicates a spatiotemporal specialization of ERK activity that is in part dependent on the stimulatory context.

We identify pro-inflammatory conditions including IL-1β, lL-6, TNF-α, and IFN-γ, that increase the frequency of SPREADs through secreted EGFR and IL6R ligands. Our findings suggest a novel mechanism by which cytokine-mediated ERK activity can cause collective cell behavior in the airway epithelium that differs from canonical EGF-mediated ERK signaling. We propose that localized SPREAD events in specific areas caused by exposure to pro-inflammatory ligands may be a mechanism for targeted ERK-mediated airway barrier permeabilization. SPREADs caused by localized cytokine secretion in the lung epithelium could synchronize barrier permeability (5, 13) with cytokine-mediated chemoattraction of innate and adaptive immune cells at specific sites, providing an entry mechanism for immune cells while also possibly mitigating the ensuing damage to the airway epithelium caused by influxing inflammatory cells. This proposed mechanism is distinct compared to the barrier-protective effects of EGF-mediated ERK activity (51), which we demonstrate to be uniformly distributed in epithelial monolayers. Localized changes in epithelial plasticity mediated by ERK have also been observed in Drosophila and zebrafish models (52, 53).

Our study adds to the growing body of literature that underscores the importance of spatial signaling in maintaining proper epithelial homeostasis. A low frequency of SPREADs is important for epithelial homeostasis, specifically tuning cell survival and apoptosis rates to the local context of each cell and allowing the tissue to adapt to cell death (20) and division events (19). On the other hand, continuous high frequency

SPREAD events, such as those caused by pro-inflammatory cytokines, might have deleterious effects on the epithelium by triggering a positive feedback loop of epithelial permeability and immune cell recruitment. Beyond ERK, multiple pathways could exhibit SPREAD-like behavior and collectively influence tissue systems. For example, calcium waves from Caspase-8-expressing cells or a laser-ablated apoptotic cell in zebrafish promote RAS-mutant MDCK cell ejection (54). Locally released cytokines such as IL-1β or TNF-α can propagate signals between immune cells and epithelial cells through the NF-κB and JNK pathways (55). Collectively, these ligands, receptors, and pathways allow for a complex spatiotemporal flow of information regulating cell behavior. Our study highlights how methods with high spatial and temporal resolution can be used to understand how these pathways operate in multicellular systems such as the airway epithelium.

Our observations that cytokine signaling, hydrocortisone, and metabolic conditions all modulate SPREAD frequency are consistent with their known roles in inflammation. However, we also provide for the first-time evidence that these factors operate, at least in part, through the shared mechanism of ERK SPREADs. This convergence suggests that future studies evaluating possible synergistic effects of anti-cytokine drugs, metabolic inhibitors (e.g., metformin), and anti-inflammatory drugs (e.g., corticosteroids, statins) may reveal combinations of treatments with clinical utility in a manner not previously imagined. It may also be possible to identify clinical alternatives for patients who are resistant to SPREAD modulation through one mechanism (e.g., corticosteroids) but sensitive through another (e.g., metformin, statins, phosphodiesterase-4 inhibitors, leukotriene receptor antagonists, etc.). While biosensors cannot be used directly in

human patients, they could feasibly be applied to primary human airway epithelial tissue from donors. SPREAD mechanisms could thus be assessed in individual patients as part of a precision medicine approach to the mucosal innate immune response.

In conclusion, our findings indicate that pro-inflammatory cytokines induce SPREADs in airway epithelial cells, and that SPREADs play an important role in coordinating the response of airway epithelial cells to changes in their environment, particularly in conditions where airway epithelial barrier breakdown is observed. These findings contribute to our understanding of the complex signaling networks that regulate the response of lung epithelial cells during inflammation, and show a novel mechanism of airway disease progression, and provide insights into potential therapeutic targets for airway diseases associated with ERK signaling and barrier dysfunction.

TABLE 1: Groups of pro-inflammatory conditions tested.

Common Name:	Inflammatory Ligand(s):
Asthma - Type 1 (Non-Type 2)	IFN-γ and TNF-α
Asthma - Type 2	IL-4, IL-5, (IL-9), IL-13
Asthma - Neutrophilic	IL-17a, IL-23
Systemic Metabolic Inflammation	IL-1β, IL-6, and TNF-α
Bacterial Infection	LPS
Viral Infection	Poly I:C and IFN-γ

FIGURES

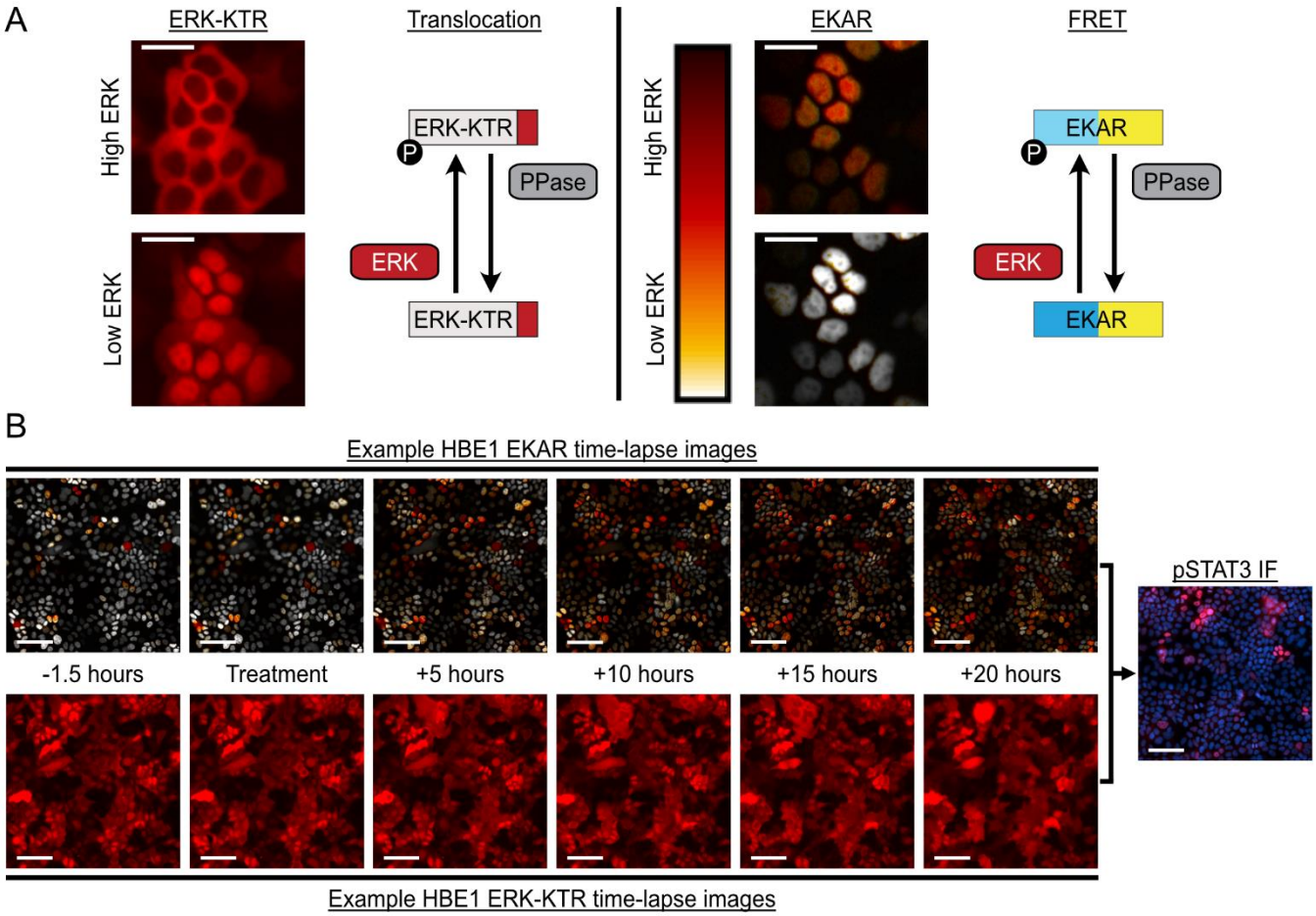

Figure 1. ERK biosensor diagrams, and example images. (A) Example images of HBE1 cells expressing fluorescent biosensors for ERK activity, with the top image showing near-maximal ERK activity (EGF stimulation) and the bottom image showing near-minimal activity (MEK inhibitor). *Left,* ERK-KTR (translocation reporter) localizes to the cytoplasm upon ERK activation and to the nucleus upon ERK inhibition. *Right*, EKAREN4 (FRET reporter) shows a high FRET signal upon ERK activation and a low FRET signal upon inhibition. Scale bars, 25 μm. **(B)** Example time lapse images of HBE1 cells expressing both the ERK-KTR and EKAREN4 biosensors. Right panel: for certain experiments, cells were fixed following live-cell imaging of the biosensor and stained for pSTAT3 (red) and DNA (blue). Scale bars, 100 μm.

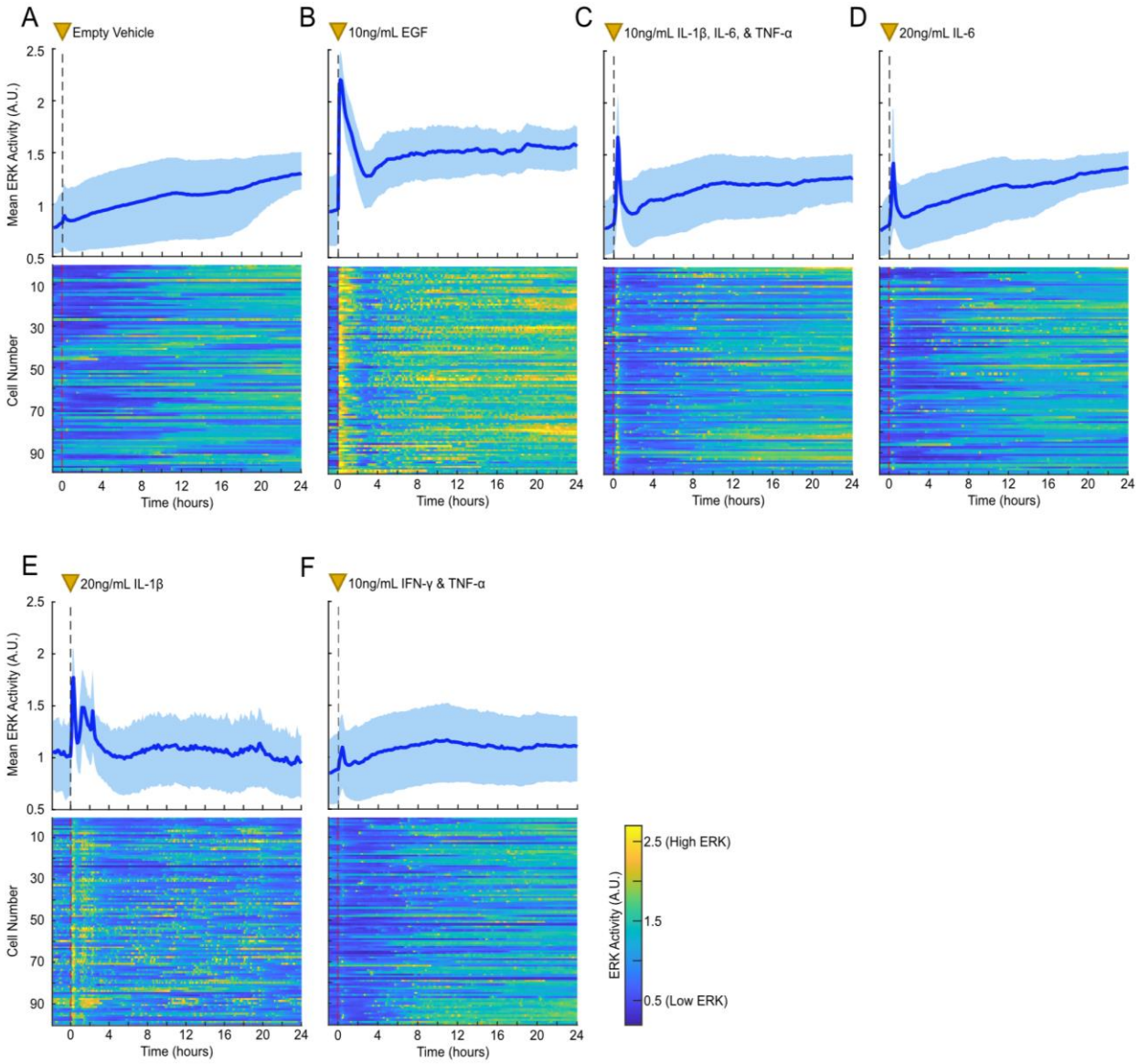

Figure 2. ERK activity of HBE1 cells in response to vehicle control, EGF, or pro-inflammatory ligands. (A-F) The top panels show the mean ERK-KTR signal (dark blue line) with 25th/75th quantiles (shaded light blue regions). The bottom panels show heatmaps of ERK activity (color axis) for 100 randomly selected cells. Each horizontal row depicts one cell's activity over time. Heatmaps show representative data from 1 of 3 technical replicates, >500 cells per condition. The dashed vertical lines and yellow triangles (0 hours on the time axis) indicate when treatments (listed next to the yellow triangles) were applied to the cells.

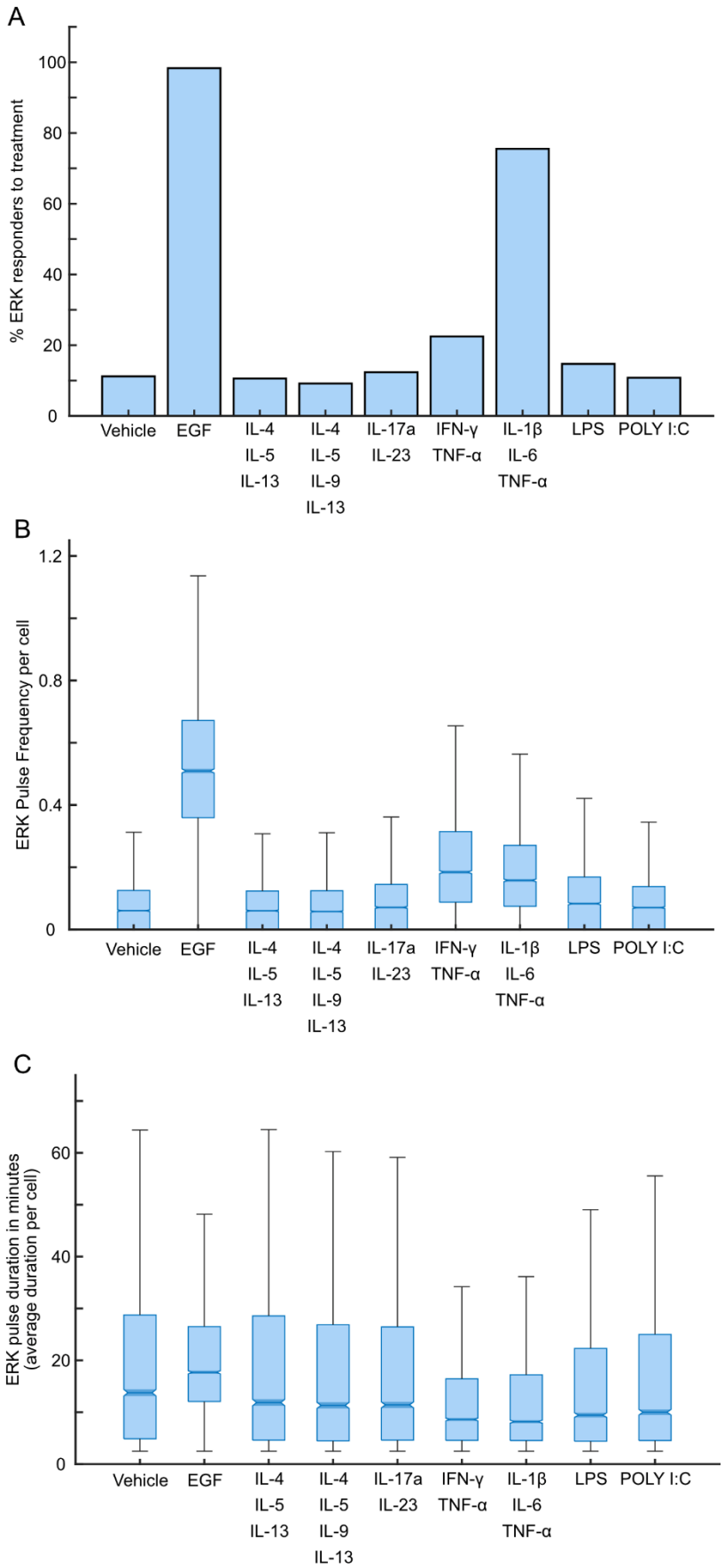

Figure E1. Quantification of ERK activity in HBE1 cells in response to pro-inflammatory ligands and controls. **(A)** The percentage of cells that respond to respective treatments. Responders were defined as cells that increase in ERK-KTR signal by 0.3 A.U. after treatment, relative to mean activity 1 hour before treatment. **(B)** Notched box plots of ERK pulse frequency over 24 hours following treatment (occurrences of ERK activation per cell per hour) for each condition. Plots represent the median (line at center of notch), 95% confidence interval of the mean (notch), interquartile range (25^{th}-75^{th} percentile, blue box), and range of data excluding outliers (whiskers). **(C)** Notched box plots showing each cell's average ERK pulse duration (in minutes). Data for A-C is cumulative from at least 3 experimental replicates, 9 technical replicates, and >2,000 cells per condition.

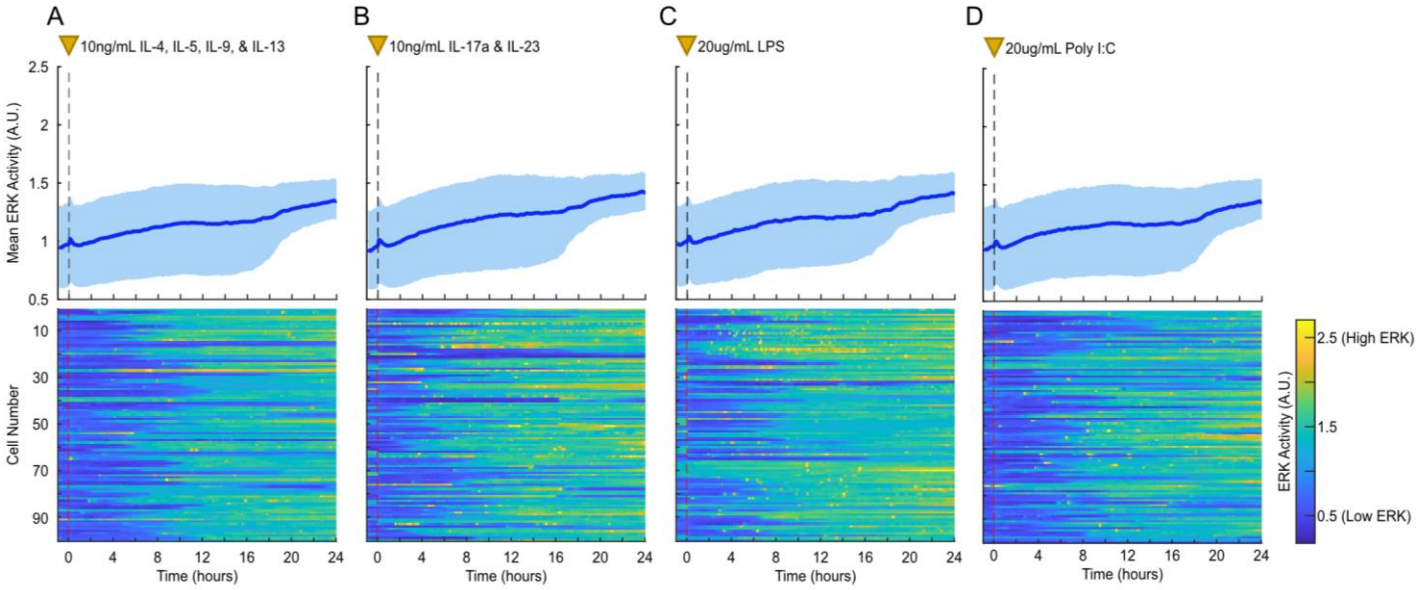

Figure E2: ERK responses of HBE1 cells to pro-inflammatory ligands. (A-D) Mean and heatmap plots showing HBE1 cell ERK activity in response to pro-inflammatory ligands and vehicle control. Treatments occur at 0 hours, indicated by a vertical dashed line and yellow triangle. Heatmaps show ERK activity (color-axis) of 100 randomly selected cells from the data that make up the mean data plots shown above. Heatmap plots are representative data from 1 of 3 technical replicates, with >500 cells per condition.

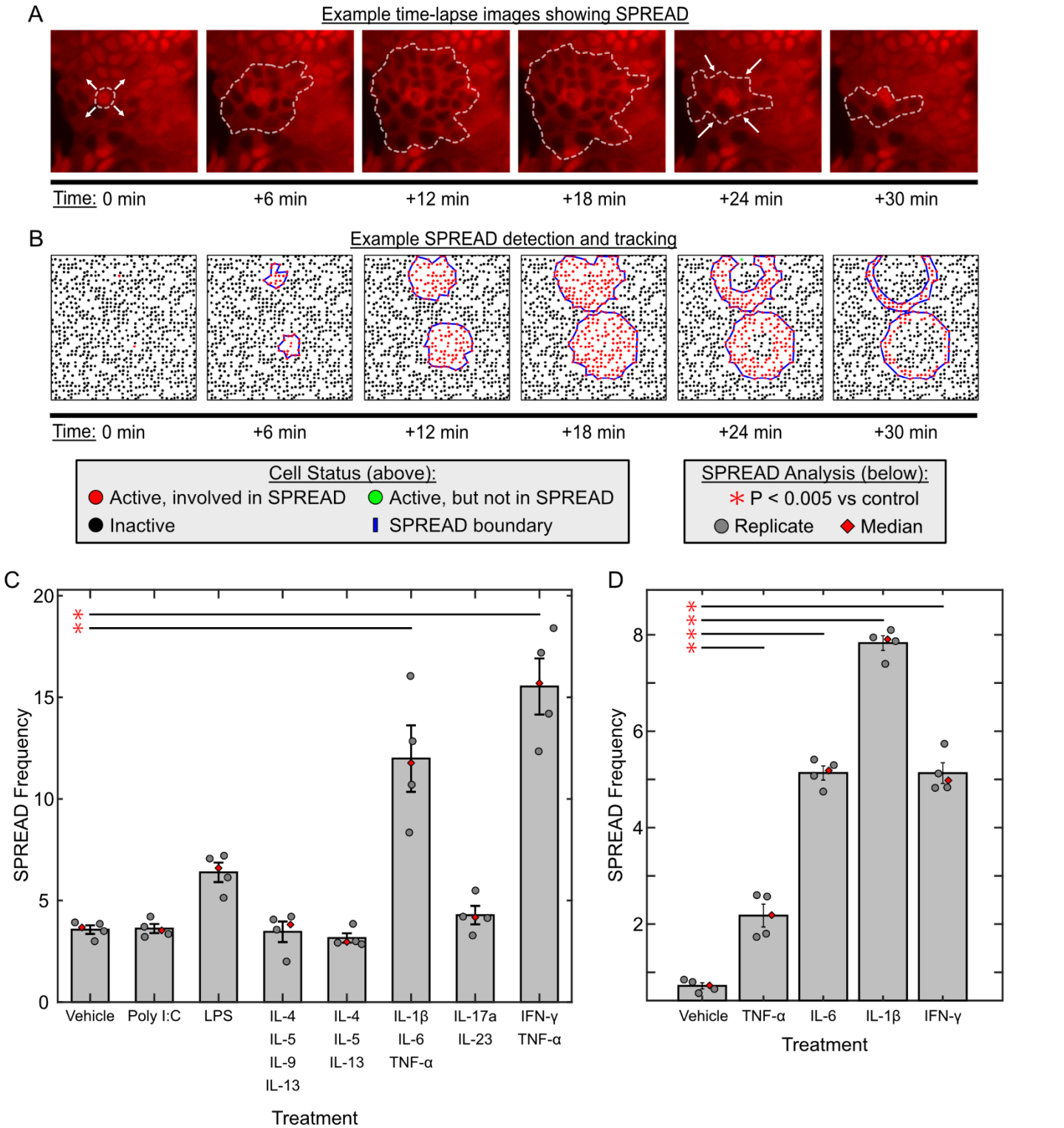

Figure 3: Spatially localized ERK activity in HBE1 cells in response to pro-inflammatory ligands. (A) Time lapse images showing an example ERK activity wave (SPREAD) occurring in HBE1 cells. The dashed white line indicates the edge of a SPREAD event, and the white arrows represent the direction of SPREAD growth or shrinkage. Time 0 indicates the initiation point of the example SPREAD, approximately 16 hours after treatment with 10 ng/mL IL-1β. **(B)** SPREAD detection results on simulated ERK activity data. Red dots represent active cells identified to be part of a SPREAD. Blue

solid lines show the boundary of detected SPREADs. Black dots represent inactive cells. Green dots show cells that are considered to have active ERK, but are not a part of a detected SPREAD. **(C and D)** SPREAD frequency (SPREAD occurrences per hour, normalized to mm^2) in the 24 hours following treatment with the indicated stimuli. Gray dots represent technical replicates, red diamonds show the median, and error bars show S.E.M.. Red asterisks and lines indicate conditions where SPREAD frequency is significantly different compared to the control group ($P < 0.005$), calculated using 1-way ANOVA compared to the control and adjusted for multiple comparisons via the Dunnett's procedure.

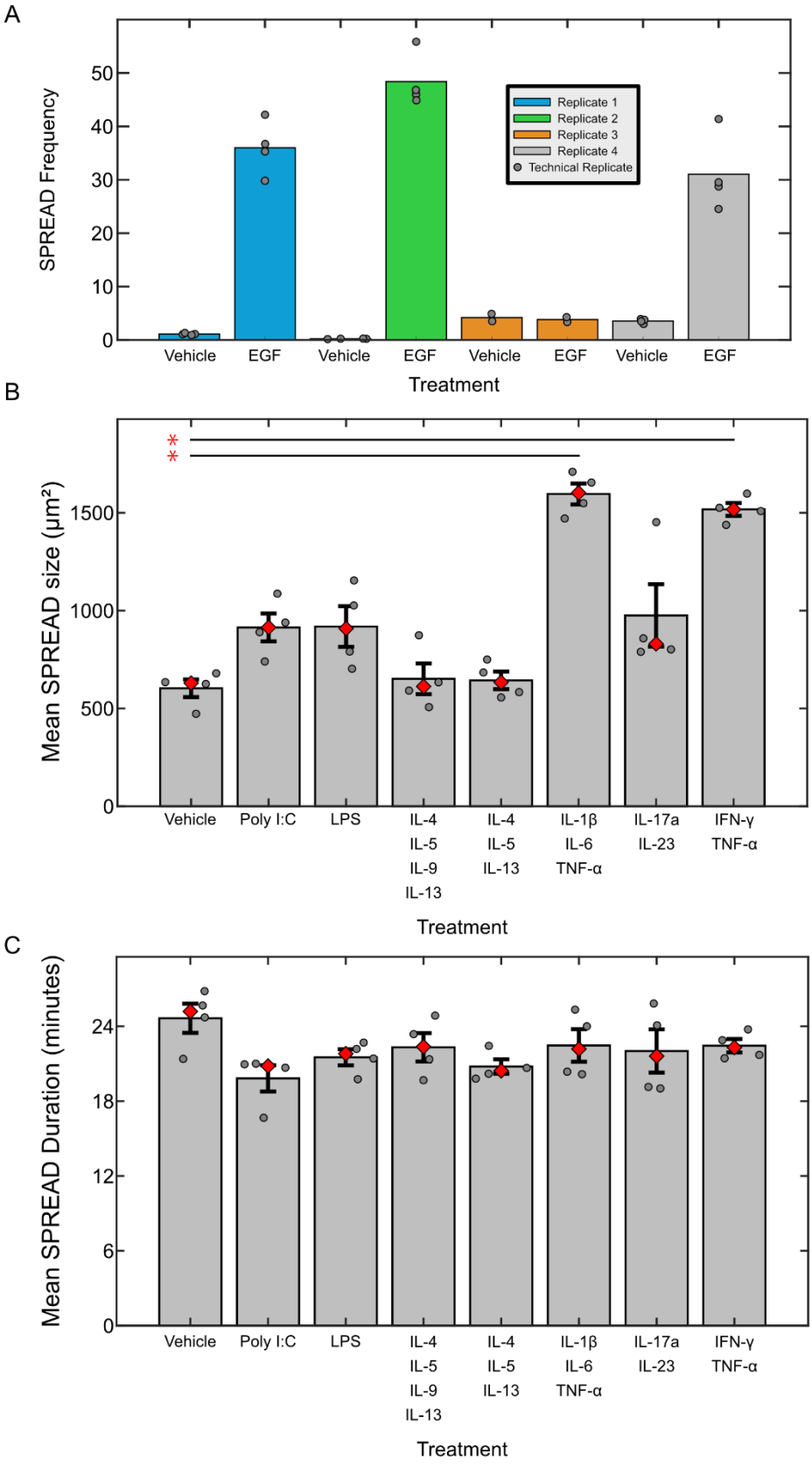

Figure E3: Variable SPREAD recognition in EGF treated cells and pro-inflammatory ligands-induced SPREAD size and duration in HBE1 cells. (A) SPREAD frequency in vehicle and EGF treated HBE1 cells compared across experimental replicates. Dark gray dots represent technical replicates within experimental replicates. **(B)** Means of SPREAD sizes (maximum radius reached per SPREAD, in μm^2) plotted according to treatment. **(C)** Mean SPREAD duration (in minutes) by treatment. For both C and D, dark gray dots represent technical replicates, red diamonds indicate data median, and error bars show S.E.M.. Red asterisks and lines indicate conditions where SPREAD duration is significantly different compared to vehicle control group ($P < 0.005$), calculated using 1-way ANOVA compared to the control and adjusted for multiple comparisons via the Dunnett's procedure.

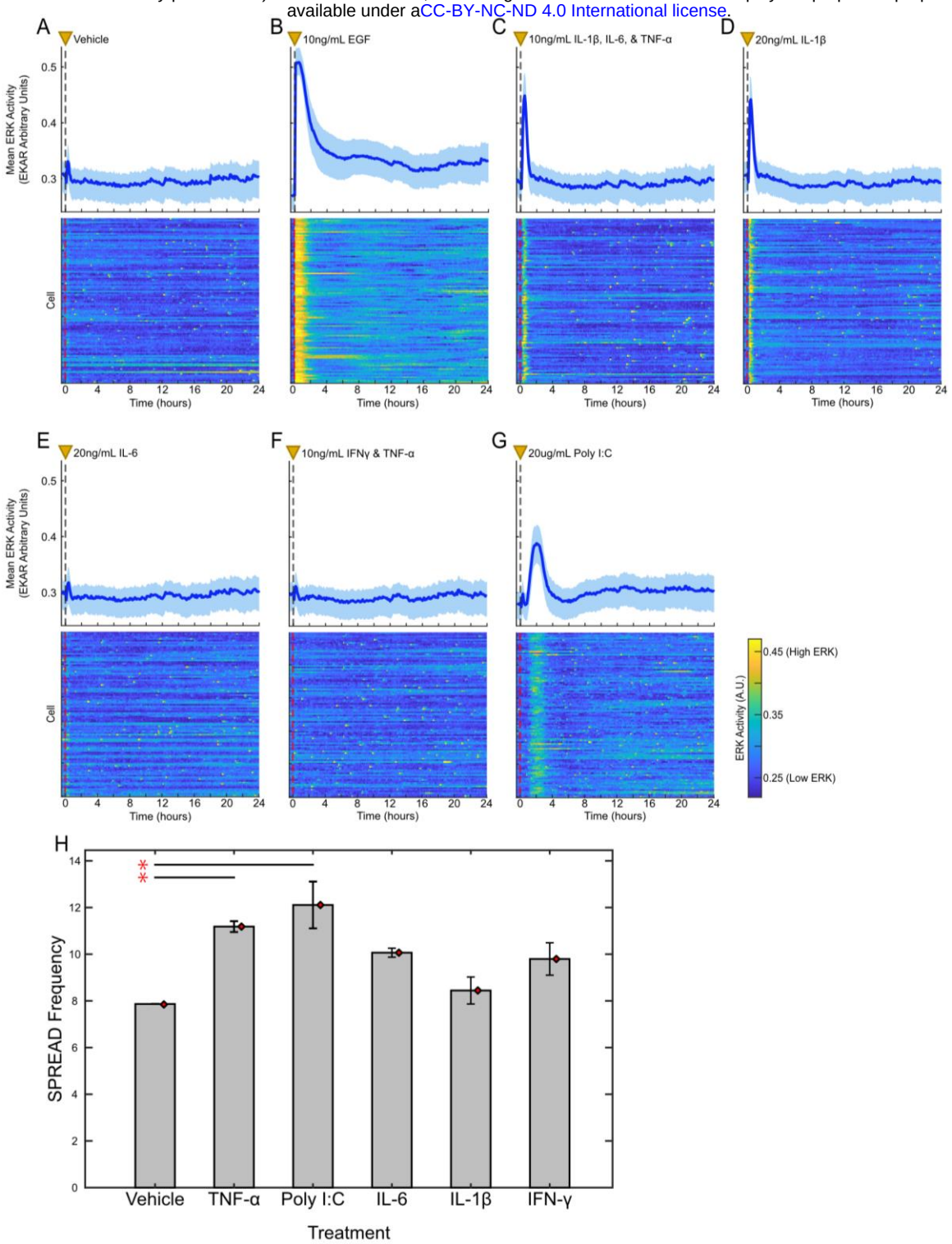

Figure 4. Pro-inflammatory ligands increase ERK activity in 16HBE cells. (A-G) Mean and interquartile range (25th-75th) of EKAREN4 signal in response to vehicle, EGF, or pro-inflammatory cytokines treatment over time. Dashed lines with yellow triangles indicate treatment (time 0 hour). **(H)** SPREAD frequency (SPREAD occurrences per hour, normalized to mm^2) within the 24 hours following treatment. Gray bars show the mean, and red diamonds the median, of three technical replicates. Error bars show S.E.M. Red asterisks indicate conditions where SPREAD frequency is significantly different compared to the control group ($P < 0.005$), calculated via 1-way ANOVA compared to the control and adjusted for multiple comparisons via Dunnett's procedure.

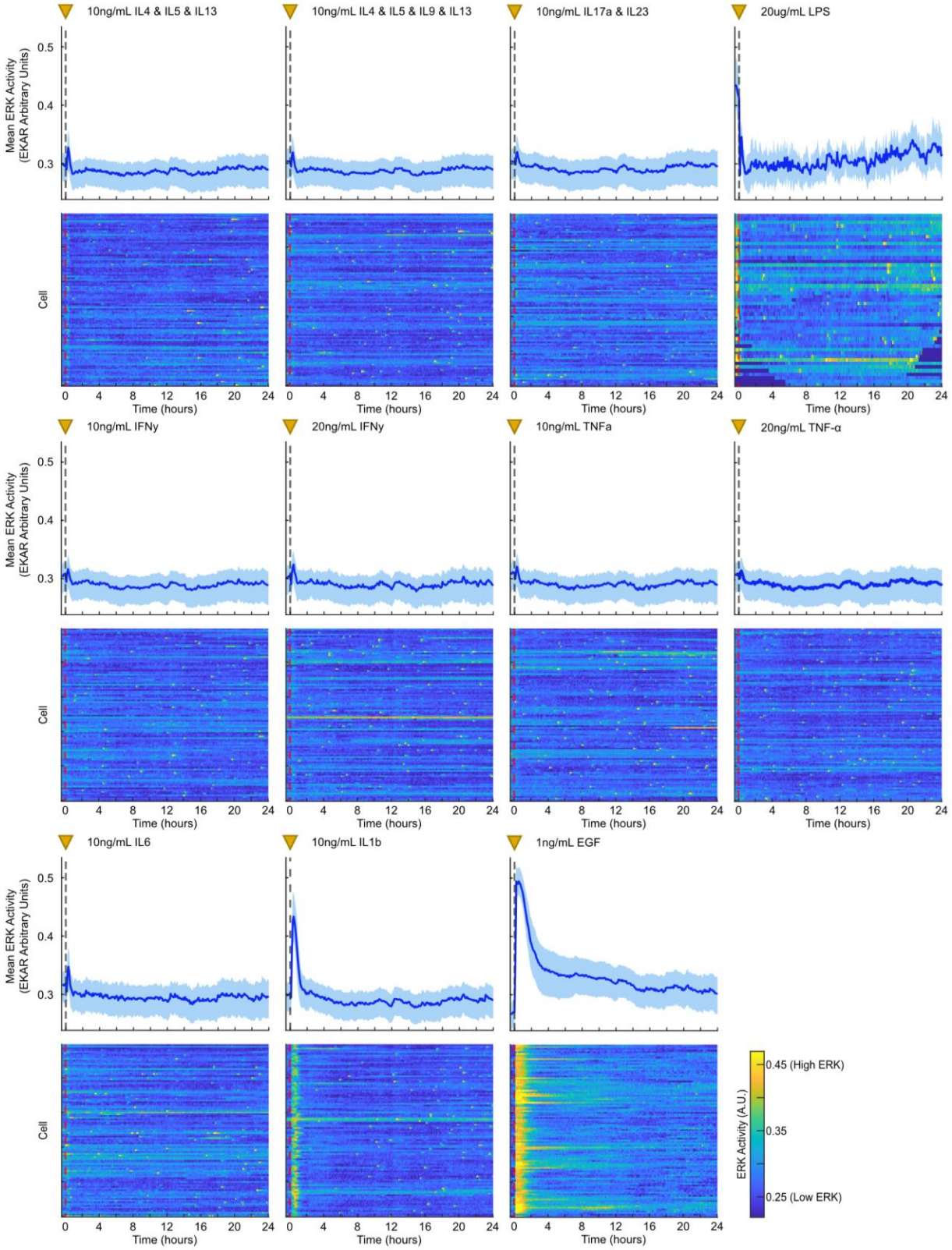

Figure E4: ERK responses of 16HBE cells to control and pro-inflammatory conditions. Top rows show mean with interquartile range of ERK activity across all cells from each condition. Heatmaps show ERK activity (color-axis) of 100 randomly selected cells from the data that make up the mean data plots above. Plots are representative data from 1 of 3 technical replicates, >500 cells per condition. Treatments occur at 0 hours, indicated by the dashed vertical lines and yellow triangles.

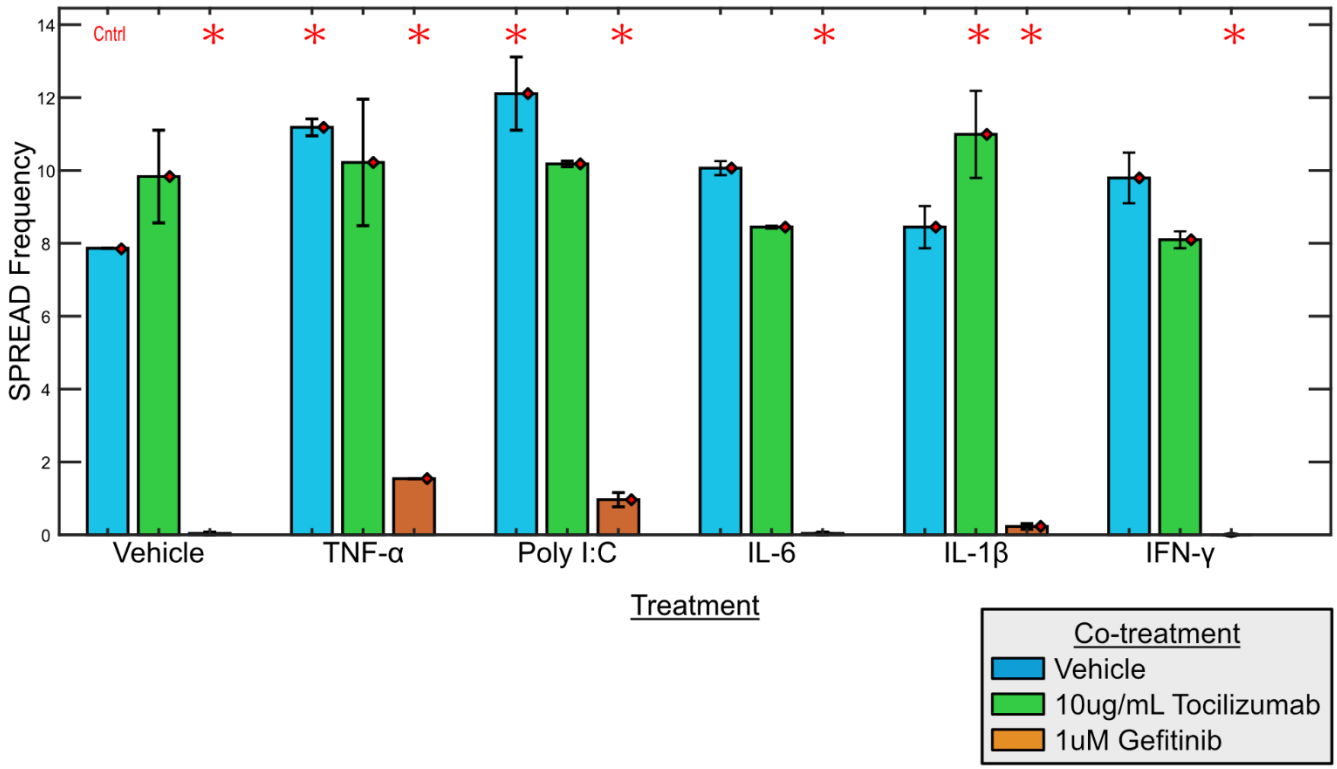

Figure E5. Receptor dependency of SPREADs in 16HBE cells. SPREAD frequency of 16HBE cells co-treated with vehicle or pro-inflammatory conditions plus vehicle, tocilizumab, or gefitinib. Bars indicate the mean and red diamonds the median of the replicates. Error bars show S.E.M. Red asterisks indicate conditions where SPREAD frequency is significantly different compared to the control group ($P < 0.005$), calculated via 1-way ANOVA compared to the control and adjusted for multiple comparisons via Dunnett's procedure.

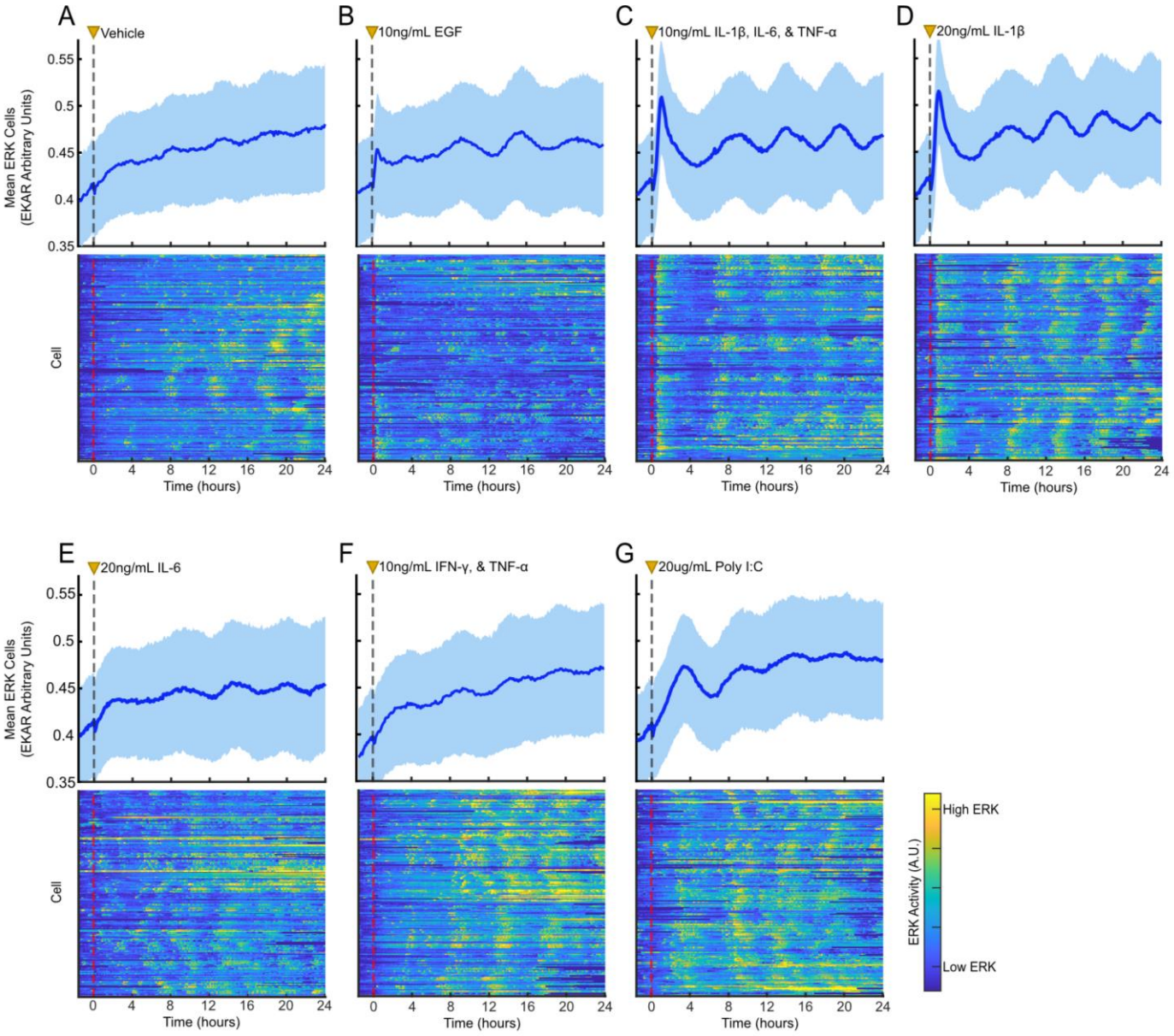

Figure 5. ERK responses of pHBE* cells following treatment with vehicle, EGF, or pro-inflammatory ligands. (A-G; *top rows*) Mean and 25th/75th quantiles of ERK activity across all cells in given treatment from representative experimental replicates (>4,000 cells per condition across 4 technical replicates). **(A-G; *bottom rows*)** Heatmaps showing normalized ERK activity (color-axis) from 200 cells within a representative technical replicate, organized such that each cell (row) is positioned next to the closest neighboring cell in physical space. Treatment occurs at hour 0 as indicated by the dashed vertical line and yellow triangle. *primary human bronchial epithelial cells in submerged culture.

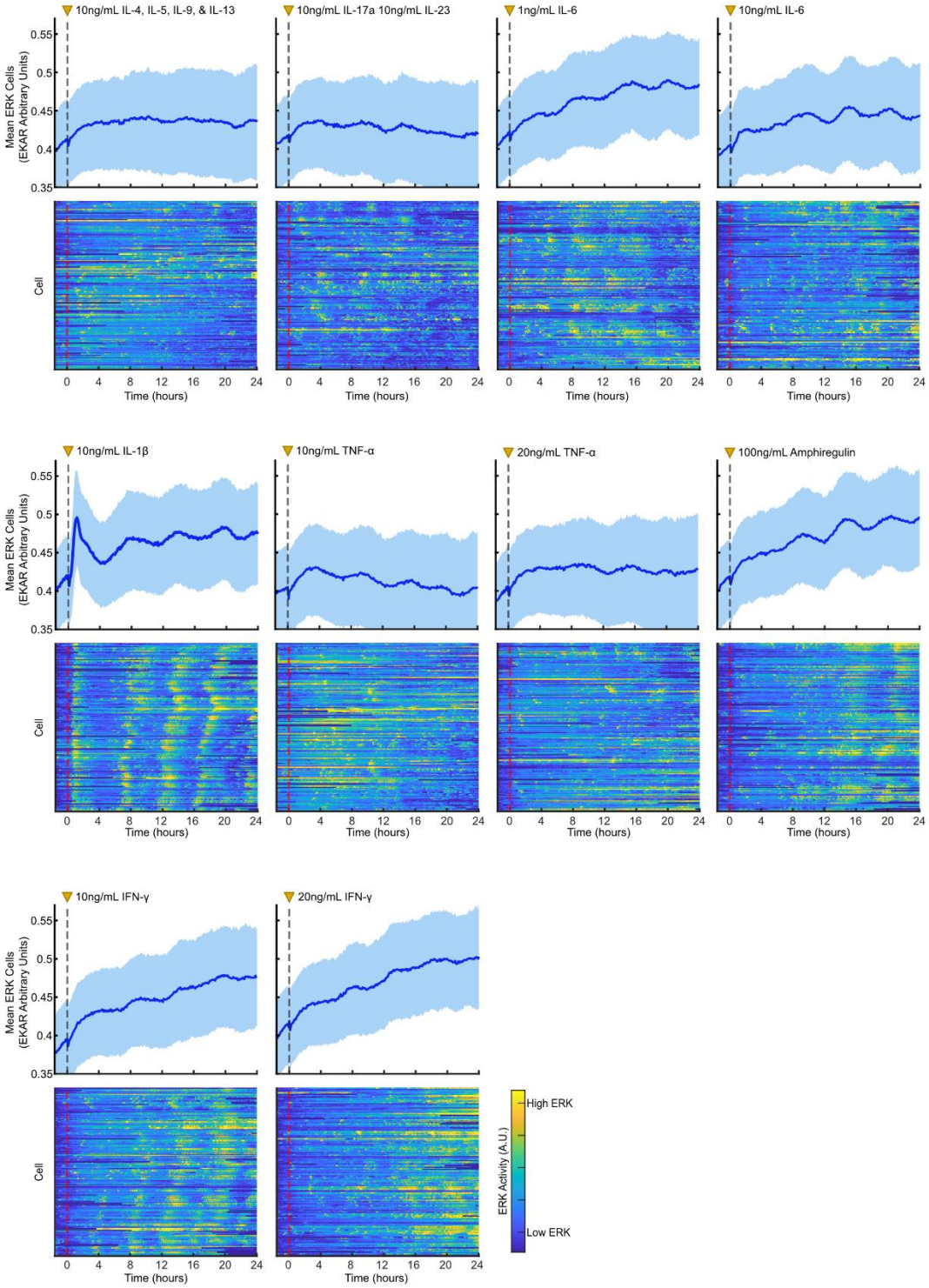

Figure E6. Mean and representative single cell ERK responses of pHBE* following treatment with pro-inflammatory conditions. (*Top rows*) Mean and 25th-75th interquartile range of ERK data (EKAREN4) across all cells in representative experimental replicates (>4,000 cells per condition across 4 technical replicates). (*Bottom rows*) Heatmaps showing normalized ERK activity (color-axis) from 200 cells within a representative technical replicate, organized such that each cell (row) is positioned next to the closest neighboring cell in physical space. Treatment occurs at hour 0 as indicated by the dashed vertical line and yellow triangle. *primary human bronchial epithelial cells in submerged culture.

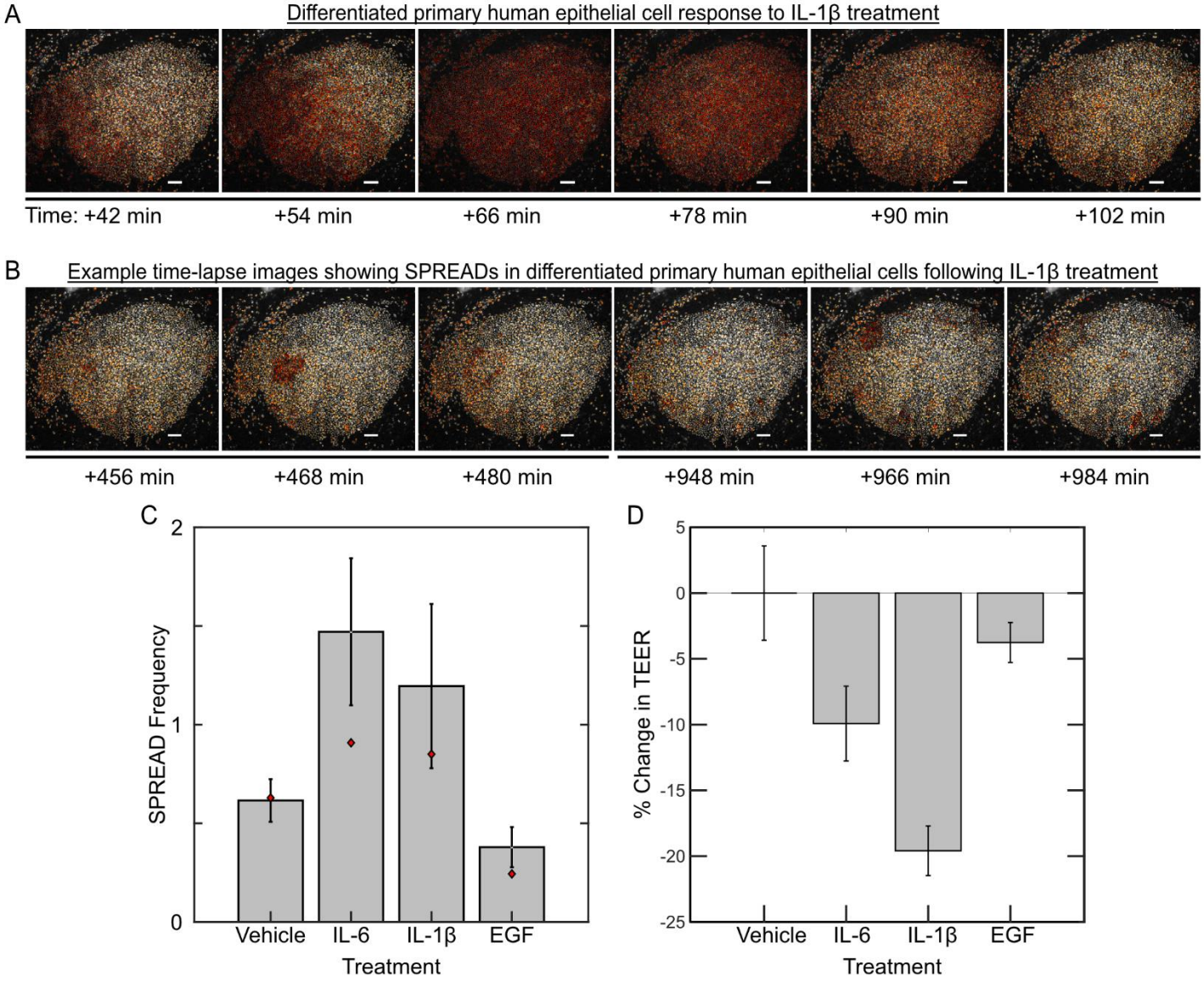

Figure 6. ERK responses to pro-inflammatory conditions in ALI-differentiated primary human bronchial epithelial (pHBE) cells. (A) Representative images showing EKAREN4 biosensor activity in response to treatment with 20 ng/mL IL-1β. **(B)** Representative image showing SPREADs occurring in differentiated pHBE cells following treatment with 20 ng/mL IL-1β. For both A and B, relative ERK activity is represented in pseudo-coloring as in Figure 1, with low relative ERK activity in white and high ERK activity in red. Time labels are relative to treatment with 20 ng/mL IL-1β at 0 minutes. Scale bar is 100 μm. **(C)** SPREAD frequency following treatment with indicated ligands. Red diamonds show the median of the data, and error bars show S.E.M. (D) Percent change in trans-epithelial resistance (TEER) following 24-hours of treatment with controls or pro-inflammatory cytokines (vehicle subtracted).

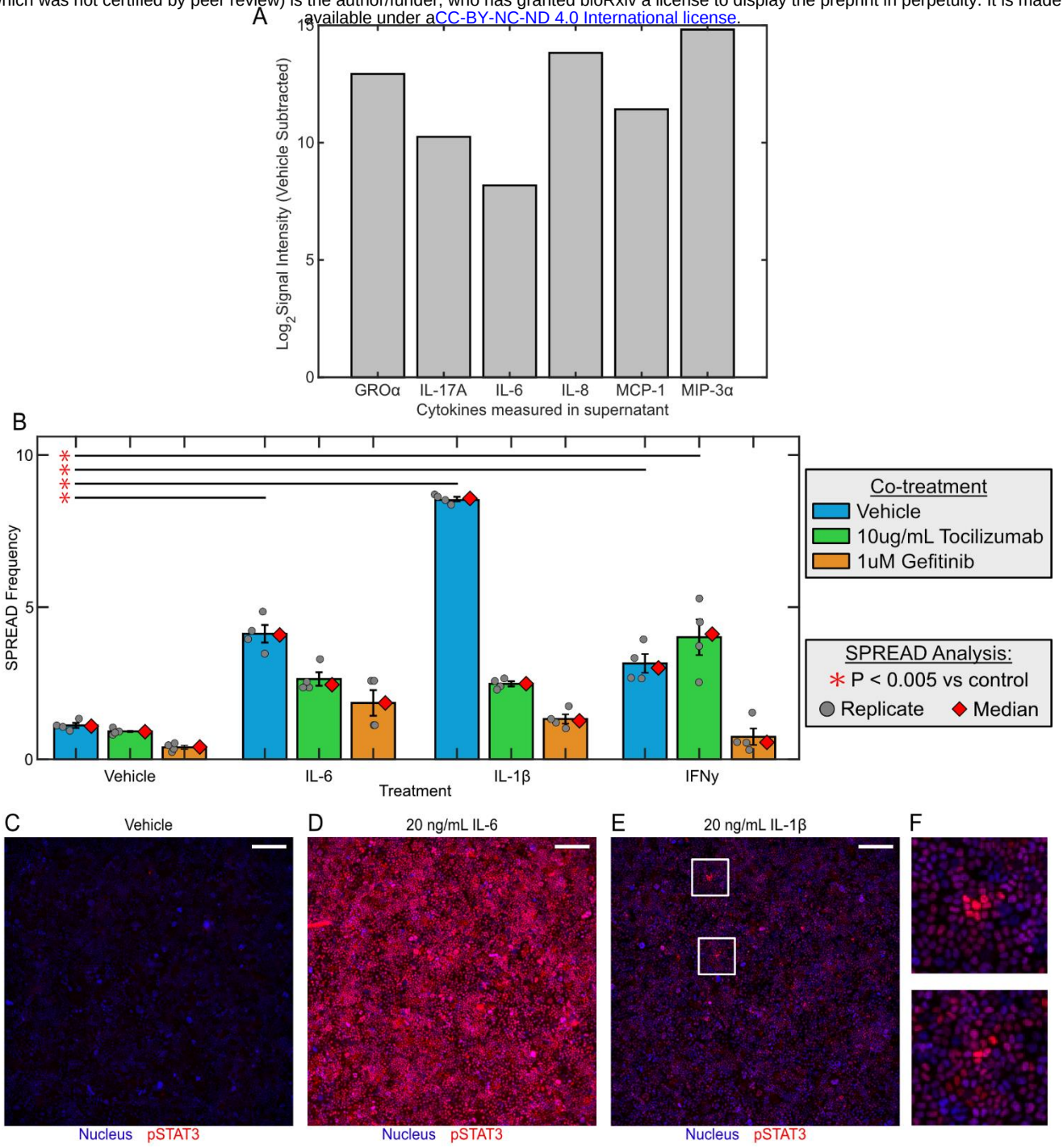

Figure 7. Investigating the mechanism of cytokine-mediated SPREADs. (A) Vehicle-subtracted Log_2 mean intensity of secreted cytokines in the supernatant of IL-1β treated HBE1 cells versus control. **(B)** SPREAD frequency of HBE1 cells co-treated with vehicle or pro-inflammatory conditions (indicated by labels under bars) plus vehicle, tocilizumab, or gefitinib (indicated by bar color). **(C-E)** pSTAT3 immunofluorescence (IF) stains of HBE1 cells after 24-hours treatment with vehicle, 20 ng/mL IL-6, or 20 ng/mL IL-1β. The nuclear marker is shown in blue with pSTAT3 shown in red. All image intensities are scaled similarly per channel. White boxes outline regions of high pSTAT3 activity in IL-1β treated cells. Representative images selected from 9 technical replicates across 3 independent experiments. Scale bars in panels C-E are 250 μm. **(F)** Enlarged images of clusters of pSTAT3 activation, identified in panel E by two white boxes. For panel F, the whole image in panel E was scaled 4x then cropped.

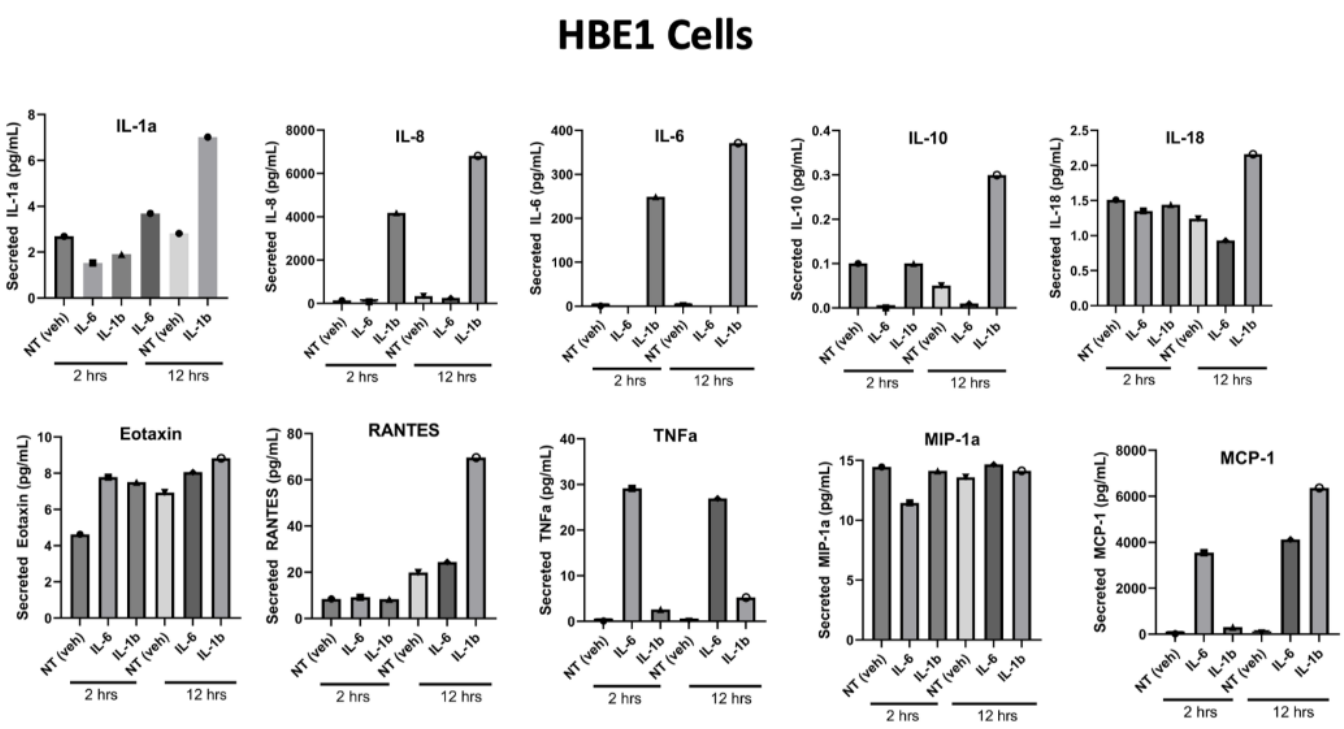

Figure E7. Luminex bead assay confirms cytokine release by HBE1 cells following IL-1β treatment. Bead-based cytokine assays for the indicated cytokines (plot titles) in cell culture supernatant from HBE1 cells treated with the cytokines listed on the horizontal axis.

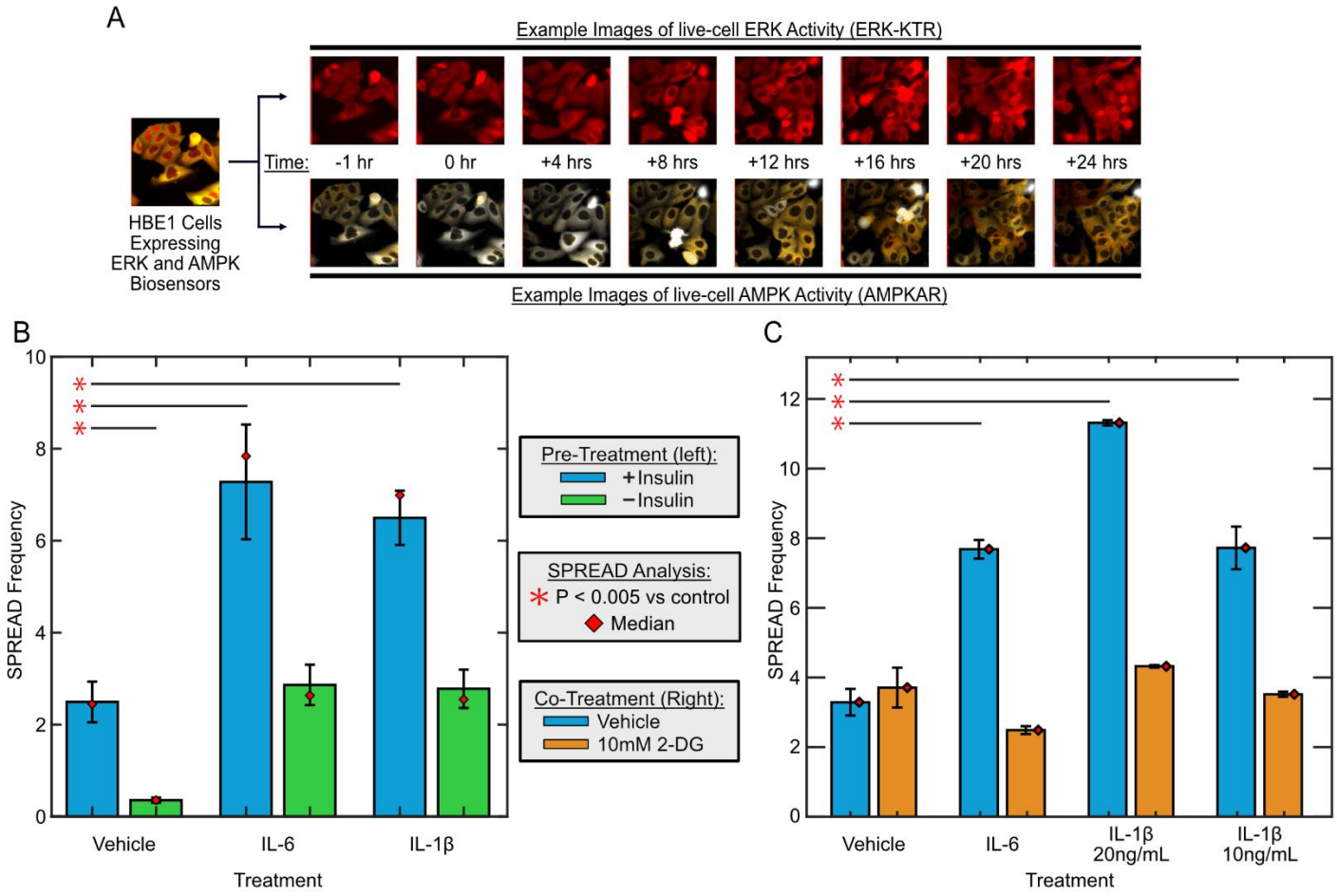

Figure 8. Metabolic regulation of cytokine-mediated SPREADs. (A) Example images of HBE1 cells expressing both the ERK and AMPK biosensor. *Top* images show ERK activity over time and bottom images show AMPK activity over time in the same cells. Cells in example images were treated with EGF and 2-DG at 0 hours. **(B)** SPREAD frequency of HBE1 cells treated with pro-inflammatory cytokines following 16 hours of either starvation or supplementation of insulin. **(C)** Comparison of the change in IL-6- and IL-1β- induced SPREAD frequency when cells are co-treated with 2-DG versus control.

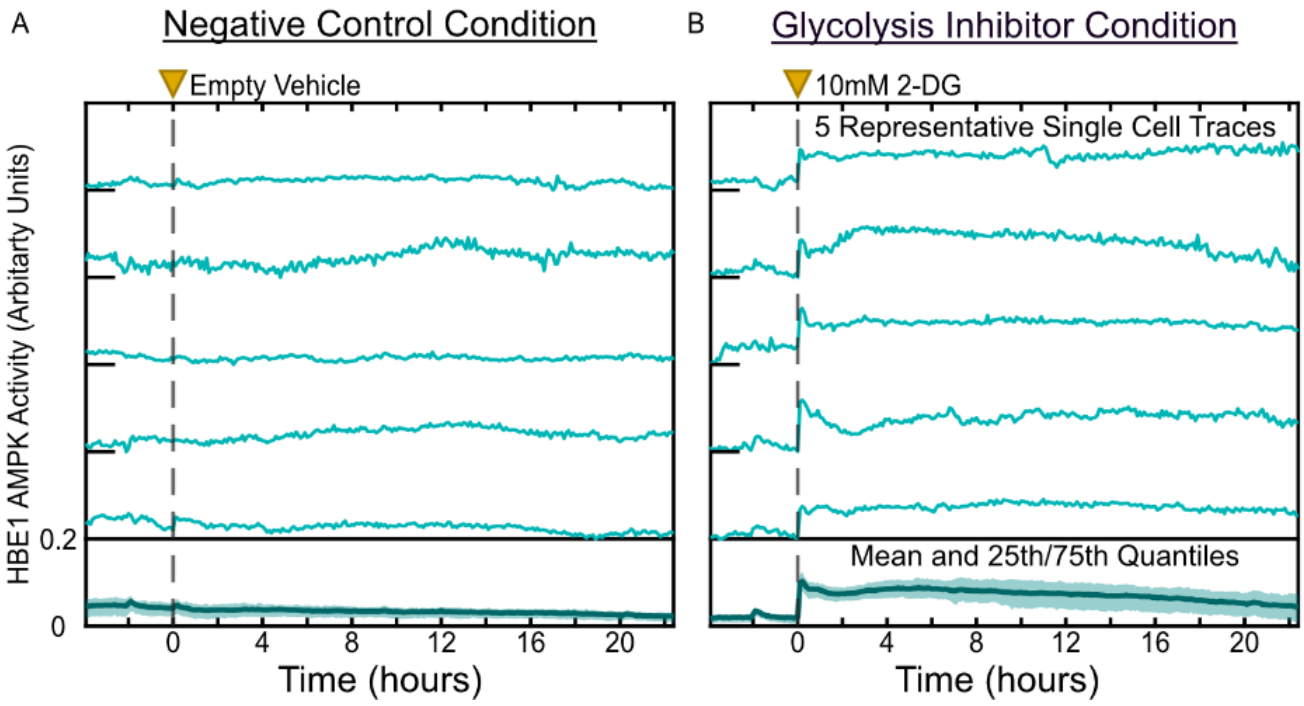

Figure E8. Verification of metabolic stress in HBE1 cells via monitoring of AMPK activity. (A and B) Five representative single cell tracks and the mean (with 25th-75th interquartile range) AMPK activity following treatment with vehicle or 10 mM 2-deoxyglucose (2-DG). Data are from 1 representative experimental replicate of 3 performed. Plots are derived from >500 cells of data per condition.

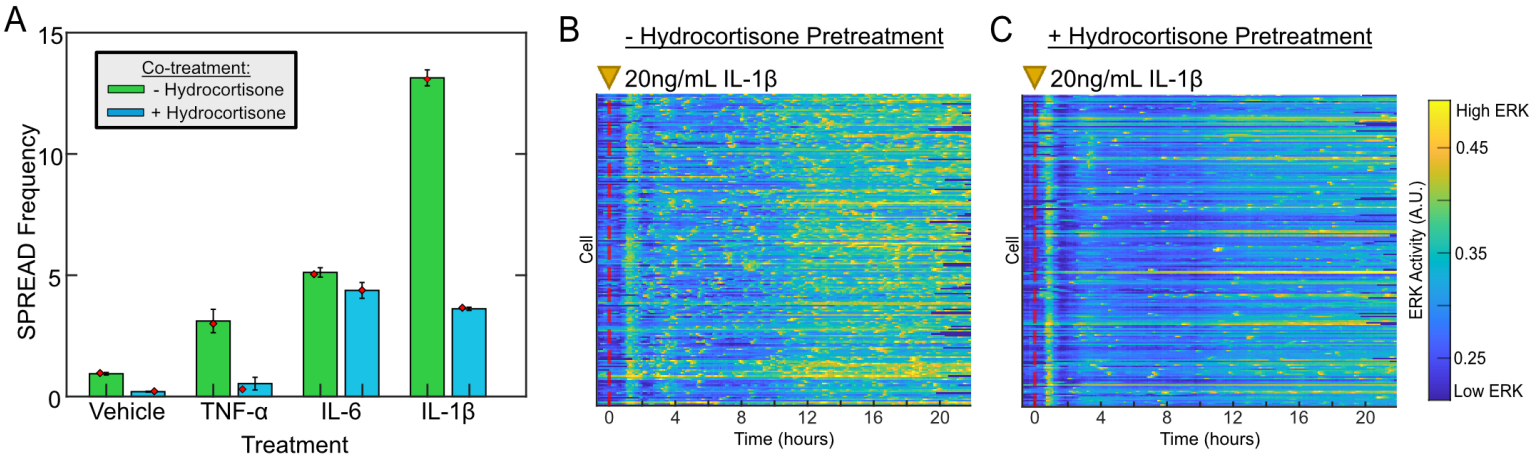

Figure 9. Corticosteroids suppress pro-inflammatory cytokine-induced SPREADs in HBE1 cells. (A) Suppression of TNFα, IL-6, IL-1β, and IFN-γ -induced SPREADs by 24-hour pre-treatment with 1.38 μM hydrocortisone. **(B and C)** Heatmaps showing ERK activity (color-axis) from 200 cells within a representative technical replicate organized such that each cell (row) is positioned next to the closest neighboring cell in physical space. 20ng/mL IL-1β treatment occurs at hour 0 as indicated by the yellow triangle and dashed line.

REFERENCES

1. Pelaia G, Cuda G, Vatrella A, Gallelli L, Caraglia M, Marra M, *et al.* Mitogen-activated protein kinases and asthma. *J Cell Physiol* 2005;202:642–653.
2. Lee PJ, Zhang X, Shan P, Ma B, Lee CG, Homer RJ, *et al.* ERK1/2 mitogen-activated protein kinase selectively mediates IL-13-induced lung inflammation and remodeling in vivo. *J Clin Invest* 2006;116:163–173.
3. Schuh K, Pahl A. Inhibition of the MAP kinase ERK protects from lipopolysaccharide-induced lung injury. *Biochem Pharmacol* 2009;77:1827–1834.
4. Madala SK, Schmidt S, Davidson C, Ikegami M, Wert S, Hardie WD. MEK-ERK pathway modulation ameliorates pulmonary fibrosis associated with epidermal growth factor receptor activation. *Am J Respir Cell Mol Biol* 2012;46:380–388.
5. Petecchia L, Sabatini F, Usai C, Caci E, Varesio L, Rossi GA. Cytokines induce tight junction disassembly in airway cells via an EGFR-dependent MAPK/ERK1/2-pathway. *Lab Invest* 2012;92:1140–1148.
6. Rezaee F, Georas SN. Breaking barriers. New insights into airway epithelial barrier function in health and disease. *Am J Respir Cell Mol Biol* 2014;50:857–869.
7. Khorasanizadeh M, Eskian M, Gelfand EW, Rezaei N. Mitogen-activated protein kinases as therapeutic targets for asthma. *Pharmacol Ther* 2017;174:112–126.
8. Liu J, Li YY, Andiappan AK, Yan Y, Tan KS, Ong HH, *et al.* Role of IL-13Rα2 in modulating IL-13-induced MUC5AC and ciliary changes in healthy and CRSwNP mucosa. *Allergy* 2018;73:1673–1685.
9. Moonwiriyakit A, Koval M, Muanprasat C. Pharmacological stimulation of G-protein coupled receptor 40 alleviates cytokine-induced epithelial barrier disruption in airway epithelial Calu-3 cells. *Int Immunopharmacol* 2019;73:353–361.
10. Su Y, Han W, Kovacs-Kasa A, Verin AD, Kovacs L. HDAC6 Activates ERK in Airway and

Pulmonary Vascular Remodeling of Chronic Obstructive Pulmonary Disease. *Am J Respir Cell Mol Biol* 2021;65:603–614.

11. Shah SD, Nayak AP, Sharma P, Villalba DR, Addya S, Huang W, *et al.* Targeted Inhibition of Select ERK1/2 Functions Mitigates Pathological Features of Asthma in Mice. *Am J Respir Cell Mol Biol* 2022;doi:10.1165/rcmb.2022-0110OC.
12. Handly LN, Wollman R. Wound-induced Ca2+ wave propagates through a simple release and diffusion mechanism. *Mol Biol Cell* 2017;28:1457–1466.
13. Suzuki T, Yoshinaga N, Tanabe S. Interleukin-6 (IL-6) regulates claudin-2 expression and tight junction permeability in intestinal epithelium. *J Biol Chem* 2011;286:31263–31271.
14. Serikov VB, Choi H, Chmiel KJ, Wu R, Widdicombe JH. Activation of extracellular regulated kinases is required for the increase in airway epithelial permeability during leukocyte transmigration. *Am J Respir Cell Mol Biol* 2004;30:261–270.
15. Lucas RM, Luo L, Stow JL. ERK1/2 in immune signalling. *Biochem Soc Trans* 2022;50:1341–1352.
16. van 't Wout EFA, Dickens JA, van Schadewijk A, Haq I, Kwok HF, Ordóñez A, *et al.* Increased ERK signalling promotes inflammatory signalling in primary airway epithelial cells expressing Z α1-antitrypsin. *Hum Mol Genet* 2014;23:929–941.
17. Nakamura A, Goto Y, Kondo Y, Aoki K. Shedding light on developmental ERK signaling with genetically encoded biosensors. *Development* 2021;148.:
18. Aoki K, Kumagai Y, Sakurai A, Komatsu N, Fujita Y, Shionyu C, *et al.* Stochastic ERK activation induced by noise and cell-to-cell propagation regulates cell density-dependent proliferation. *Mol Cell* 2013;52:529–540.
19. Hiratsuka T, Fujita Y, Naoki H, Aoki K, Kamioka Y, Matsuda M. Intercellular propagation of extracellular signal-regulated kinase activation revealed by in vivo imaging of mouse skin. *Elife* 2015;4:e05178.
20. Gagliardi PA, Dobrzyński M, Jacques M-A, Dessauges C, Ender P, Blum Y, *et al.* Collective

ERK/Akt activity waves orchestrate epithelial homeostasis by driving apoptosis-induced survival. *Dev Cell* 2021;56:1712–1726.e6.

21. Aikin TJ, Peterson AF, Pokrass MJ, Clark HR, Regot S. MAPK activity dynamics regulate non-cell autonomous effects of oncogene expression. *Elife* 2020;9.:
22. Yankaskas JR, Haizlip JE, Conrad M, Koval D, Lazarowski E, Paradiso AM, *et al.* Papilloma virus immortalized tracheal epithelial cells retain a well-differentiated phenotype. *Am J Physiol* 1993;264:C1219–30.
23. Bratt JM, Chang KY, Rabowsky M, Franzi LM, Ott SP, Filosto S, *et al.* Farnesyltransferase Inhibition Exacerbates Eosinophilic Inflammation and Airway Hyperreactivity in Mice with Experimental Asthma: The Complex Roles of Ras GTPase and Farnesylpyrophosphate in Type 2 Allergic Inflammation. *J Immunol* 2018;200:3840–3856.
24. Cozens AL, Yezzi MJ, Kunzelmann K, Ohrui T, Chin L, Eng K, *et al.* CFTR expression and chloride secretion in polarized immortal human bronchial epithelial cells. *Am J Respir Cell Mol Biol* 1994;10:38–47.
25. Robinson CB, Wu R. Culture of conducting airway epithelial cells in serum-free medium. *J Tissue Cult Methods* 1991;13:95–102.
26. Regot S, Hughey JJ, Bajar BT, Carrasco S, Covert MW. High-sensitivity measurements of multiple kinase activities in live single cells. *Cell* 2014;157:1724–1734.
27. Ponsioen B, Post JB, Buissant des Amorie JR, Laskaris D, van Ineveld RL, Kersten S, *et al.* Quantifying single-cell ERK dynamics in colorectal cancer organoids reveals EGFR as an amplifier of oncogenic MAPK pathway signalling. *Nat Cell Biol* 2021;23:377–390.
28. Albeck JG, Pargett M, Davies AE. Experimental and engineering approaches to intracellular communication. *Essays Biochem* 2018;62:515–524.
29. Pargett M, Gillies TE, Teragawa CK, Sparta B, Albeck JG. Single-Cell Imaging of ERK Signaling Using Fluorescent Biosensors. In: Tan A-C, Huang PH, editors. *Kinase Signaling Networks* New York, NY: Springer New York; 2017. p. 35–59.

30. Pargett M, Albeck JG. Live-Cell Imaging and Analysis with Multiple Genetically Encoded Reporters. *Curr Protoc Cell Biol* 2018;78:4.36.1–4.36.19.
31. Gillies TE, Pargett M, Minguet M, Davies AE, Albeck JG. Linear Integration of ERK Activity Predominates over Persistence Detection in Fra-1 Regulation. *Cell Syst* 2017;5:549–563.e5.
32. Gagliardi PA, Grädel B, Jacques M-A, Hinderling L, Ender P, Cohen AR, *et al.* Automatic detection of spatio-temporal signaling patterns in cell collectives. *J Cell Biol* 2023;222.:
33. Barnett KC, Xie Y, Asakura T, Song D, Liang K, Taft-Benz SA, *et al.* An epithelial-immune circuit amplifies inflammasome and IL-6 responses to SARS-CoV-2. *Cell Host Microbe* 2023;31:243–259.e6.
34. Jones SA, Scheller J, Rose-John S. Therapeutic strategies for the clinical blockade of IL-6/gp130 signaling. *J Clin Invest* 2011;121:3375–3383.
35. Scheller J, Chalaris A, Schmidt-Arras D, Rose-John S. The pro- and anti-inflammatory properties of the cytokine interleukin-6. *Biochim Biophys Acta* 2011;1813:878–888.
36. Wang Y, van Boxel-Dezaire AHH, Cheon H, Yang J, Stark GR. STAT3 activation in response to IL-6 is prolonged by the binding of IL-6 receptor to EGF receptor. *Proc Natl Acad Sci U S A* 2013;110:16975–16980.
37. Heinrich PC, Behrmann I, Haan S, Hermanns HM, Müller-Newen G, Schaper F. Principles of interleukin (IL)-6-type cytokine signalling and its regulation. *Biochem J* 2003;374:1–20.
38. Goldman MD. Lung dysfunction in diabetes. *Diabetes Care* 2003;26:1915–1918.
39. Meyer KC. Diagnosis and management of interstitial lung disease. *Transl Respir Med* 2014;2:4.
40. Garmendia JV, Moreno D, Garcia AH, De Sanctis JB. Metabolic syndrome and asthma. *Recent Pat Endocr Metab Immune Drug Discov* 2014;8:60–66.
41. Loxham M, Davies DE. Phenotypic and genetic aspects of epithelial barrier function in asthmatic patients. *J Allergy Clin Immunol* 2017;139:1736–1751.

42. Ellulu MS, Patimah I, Khaza'ai H, Rahmat A, Abed Y. Obesity and inflammation: the linking mechanism and the complications. *Arch Med Sci* 2017;13:851–863.
43. Tsalamandris S, Antonopoulos AS, Oikonomou E, Papamikroulis G-A, Vogiatzi G, Papaioannou S, *et al.* The Role of Inflammation in Diabetes: Current Concepts and Future Perspectives. *Eur Cardiol* 2019;14:50–59.
44. Jeong HW, Hsu KC, Lee J-W, Ham M, Huh JY, Shin HJ, *et al.* Berberine suppresses proinflammatory responses through AMPK activation in macrophages. *Am J Physiol Endocrinol Metab* 2009;296:E955–64.
45. Mancini SJ, White AD, Bijland S, Rutherford C, Graham D, Richter EA, *et al.* Activation of AMP-activated protein kinase rapidly suppresses multiple pro-inflammatory pathways in adipocytes including IL-1 receptor-associated kinase-4 phosphorylation. *Mol Cell Endocrinol* 2017;440:44–56.
46. Confalonieri M, Urbino R, Potena A, Piattella M, Parigi P, Puccio G, *et al.* Hydrocortisone infusion for severe community-acquired pneumonia: a preliminary randomized study. *Am J Respir Crit Care Med* 2005;171:242–248.
47. Tongyoo S, Permpikul C, Mongkolpun W, Vattanavanit V, Udompanturak S, Kocak M, *et al.* Hydrocortisone treatment in early sepsis-associated acute respiratory distress syndrome: results of a randomized controlled trial. *Crit Care* 2016;20:329.
48. Levine SJ, Larivée P, Logun C, Angus CW, Shelhamer JH. Corticosteroids differentially regulate secretion of IL-6, IL-8, and G-CSF by a human bronchial epithelial cell line. *Am J Physiol* 1993;265:L360–8.
49. Quante T, Ng YC, Ramsay EE, Henness S, Allen JC, Parmentier J, *et al.* Corticosteroids reduce IL-6 in ASM cells via up-regulation of MKP-1. *Am J Respir Cell Mol Biol* 2008;39:208–217.
50. Clayton SA, Lockwood C, O'Neil JD, Daley KK, Hain S, Abdelmottaleb D, *et al.* The glucocorticoid dexamethasone inhibits HIF-1α stabilization and metabolic reprogramming in

lipopolysaccharide-stimulated primary macrophages. *discov immunol* 2023;2:kyad027.

51. Basuroy S, Seth A, Elias B, Naren AP, Rao R. MAPK interacts with occludin and mediates EGF-induced prevention of tight junction disruption by hydrogen peroxide. *Biochem J* 2006;393:69–77.
52. Ogura Y, Wen F-L, Sami MM, Shibata T, Hayashi S. A Switch-like Activation Relay of EGFR-ERK Signaling Regulates a Wave of Cellular Contractility for Epithelial Invagination. *Dev Cell* 2018;46:162–172.e5.
53. De Simone A, Evanitsky MN, Hayden L, Cox BD, Wang J, Tornini VA, *et al.* Control of osteoblast regeneration by a train of Erk activity waves. *Nature* 2021;doi:10.1038/s41586-020-03085-8.
54. Takeuchi Y, Narumi R, Akiyama R, Vitiello E, Shirai T, Tanimura N, *et al.* Calcium Wave Promotes Cell Extrusion. *Curr Biol* 2020;30:670–681.e6.
55. Lane K, Andres-Terre M, Kudo T, Monack DM, Covert MW. Escalating Threat Levels of Bacterial Infection Can Be Discriminated by Distinct MAPK and NF-κB Signaling Dynamics in Single Host Cells. *Cell Syst* 2019;8:183–196.e4.